Journal of Geophysical Research: Biogeosciences

RESEARCH ARTICLE
10.1029/2018JG004556

Environmental Controls, Emergent Scaling, and Predictions of Greenhouse Gas (GHG) Fluxes in Coastal Salt Marshes

Omar I. Abdul-Aziz[1], Khandker S. Ishtiaq[1], Jianwu Tang[2], Serena Moseman-Valtierra[3], Kevin D. Kroeger[4], Meagan Eagle Gonneea[4], Jordan Mora[5], and Kate Morkeski[6]

[1]Ecological and Water Resources Engineering Laboratory (EWREL), Department of Civil and Environmental Engineering, West Virginia University, Morgantown, WV, USA, [2]The Ecosystems Center, Marine Biological Laboratory, Woods Hole, MA, USA, [3]Department of Biological Sciences, University of Rhode Island, Kingston, RI, USA, [4]Woods Hole Coastal and Marine Science Center, U.S. Geological Survey, Woods Hole, MA, USA, [5]Waquoit Bay National Estuarine Research Reserve, Waquoit, MA, USA, [6]Department of Marine Chemistry and Geochemistry, Woods Hole Oceanographic Institution, Woods Hole, MA, USA

Abstract Coastal salt marshes play an important role in mitigating global warming by removing atmospheric carbon at a high rate. We investigated the environmental controls and emergent scaling of major greenhouse gas (GHG) fluxes such as carbon dioxide (CO_2) and methane (CH_4) in coastal salt marshes by conducting data analytics and empirical modeling. The underlying hypothesis is that the salt marsh GHG fluxes follow emergent scaling relationships with their environmental drivers, leading to parsimonious predictive models. CO_2 and CH_4 fluxes, photosynthetically active radiation (PAR), air and soil temperatures, well water level, soil moisture, and porewater pH and salinity were measured during May–October 2013 from four marshes in Waquoit Bay and adjacent estuaries, MA, USA. The salt marshes exhibited high CO_2 uptake and low CH_4 emission, which did not significantly vary with the nitrogen loading gradient (5–126 $kg \cdot ha^{-1} \cdot year^{-1}$) among the salt marshes. Soil temperature was the strongest driver of both fluxes, representing 2 and 4–5 times higher influence than PAR and salinity, respectively. Well water level, soil moisture, and pH did not have a predictive control on the GHG fluxes, although both fluxes were significantly higher during high tides than low tides. The results were leveraged to develop emergent power law-based parsimonious scaling models to accurately predict the salt marsh GHG fluxes from PAR, soil temperature, and salinity (Nash-Sutcliffe Efficiency = 0.80–0.91). The scaling models are available as a user-friendly Excel spreadsheet named Coastal Wetland GHG Model to explore scenarios of GHG fluxes in tidal marshes under a changing climate and environment.

Key Points:
- Coastal salt marshes in Cape Cod, Massachusetts, USA, exhibited high net CO_2 uptake and low CH_4 emission
- Soil temperature was the strongest driver of the GHG fluxes, which had weak linkages with well water level, soil moisture, and porewater pH
- Emergent power law-based scaling models successfully predicted the GHG fluxes from light (PAR), soil temperature, and porewater salinity

Supporting Information:
- Supporting Information S1

Correspondence to:
O. I. Abdul-Aziz,
oiabdulaziz@mail.wvu.edu;
omariaaziz@gmail.com

Citation:
Abdul-Aziz, O. I., Ishtiaq, K. S., Tang, J., Moseman-Valtierra, S., Kroeger, K. D., Gonneea, M. E., et al. (2018). Environmental controls, emergent scaling, and predictions of greenhouse gas (GHG) fluxes in coastal salt marshes. *Journal of Geophysical Research: Biogeosciences*, *123*, 2234–2256. https://doi.org/10.1029/2018JG004556

Received 20 APR 2018
Accepted 6 JUN 2018
Accepted article online 19 JUN 2018
Published online 28 JUL 2018

1. Introduction

Coastal salt marsh sediments demonstrate high carbon sequestration rates and contribute to the mitigation of climate change by removing atmospheric carbon (Bridgham et al., 2006; Mcleod et al., 2011; National Research Council, 2015). Carbon storage in marine wetlands is often referred to as *blue carbon*, which is an emerging concept for coastal management, protection, and restoration (Crooks et al., 2010; Macreadie et al., 2017; Morris et al., 2012; Nellemann & Corcoran, 2009). However, there is a knowledge gap regarding the relative controls of various environmental drivers (e.g., solar radiation, temperature, water level, soil moisture, salinity, and pH) on the major greenhouse gas (GHG) fluxes such as carbon dioxide (CO_2) and methane (CH_4) in coastal wetlands (Mcleod et al., 2011). A pivotal question is whether the salt marsh GHG fluxes (referred to as CO_2 and CH_4 fluxes in this paper) follow any emergent scaling relationships with their environmental drivers, leading to parsimonious (involving a minimum number of parameters) and potentially generalizable models across time and space. Inadequate understanding of the dominant environmental controls and scaling hinders the development of low dimensional models and engineering tools to predict the GHG fluxes and potential carbon storage. The lack of predictive models and tools hampers the development of GHG offset protocols to derive scientific guidelines for restoration, monitoring, and maintenance of tidal wetlands under a changing climate and environment.

The net ecosystem exchange (NEE) of CO_2 represents the balance between instantaneous photosynthesis and autotrophic as well as heterotrophic respiration. Wetlands are typically CO_2 sinks during the day, since photosynthetic uptake is greater than respiration, and CO_2 sources at night due to respiration in the absence of photosynthesis (Juszczak et al., 2012). Soil temperature (ST) is the most important predictor of nighttime

net ecosystem respiration for different ecosystems, including wetlands (Lloyd & Taylor, 1994; Mahecha et al., 2010; Tong et al., 2014; Xie et al., 2014). However, subject to the availability of nutrients, the daytime CO_2 uptake by wetland plants is mainly driven by photosynthetically active radiation (PAR) and temperature (Moseman-Valtierra et al., 2016). Further, the tidal cycle may contribute to the reduction of CO_2 uptake by increasing soil salinity. High salinity substantially inhibits the salt marsh photosynthesis and productivity by impacting both stomatal and mesophyll conductance (Callaway et al., 2007; Parida & Das, 2005; Pearcy & Ustin, 1984). In general, salinity is higher at the high marsh zone compared to low marsh areas because the weaker tidal flushing at higher elevations cannot remove the accumulated salt from the soil (Callaway et al., 2007).

Wetland CH_4 fluxes are produced through soil microbial processes and mediated by plant physiology (active or passive transfer of gases from soils to atmosphere) under the influence of hydroclimatic and physicochemical factors (Smith et al., 2003). Conrad (1989) described wetland CH_4 emissions to the atmosphere as an outcome of the following soil biogeochemical and ecological processes: (i) CH_4 production by methanogenic bacteria under anaerobic conditions; (ii) CH_4 oxidation by methanotrophic bacteria mainly under aerobic conditions; and (iii) CH_4 transport to the atmosphere. Much research (e.g., Nahlik & Mitsch, 2011; Turetsky et al., 2014; Whalen, 2005) has reported a positive correlation of CH_4 emissions with ST and water level for freshwater wetlands. Bartlett et al. (1987) and Poffenbarger et al. (2011) reported a strong negative correlation between CH_4 emissions and soil salinity over a gradient from freshwater to polyhaline (e.g., $>$18 ppt) tidal marshes.

Several process models are available to predict CO_2 and/or CH_4 fluxes mainly from freshwater wetlands (e.g., Cao et al., 1996; Potter, 1997; van Huissteden et al., 2006; Walter & Heimann, 2000; Zhang et al., 2002). Recent process models of freshwater wetland carbon dynamics include McGill (St-Hilaire et al., 2010), peatland DOS-TEM (Fan et al., 2013), WetQual-C (Sharifi et al., 2013), and CoupModel (Jansson, 2012). Process-based freshwater GHG flux models are typically detailed, often over-parameterized, and require data for many input variables—providing predictions with an inherent high uncertainty (e.g., Melton et al., 2013; Zhang et al., 2002). Further, it remains unclear whether the freshwater models can be directly adapted for coastal salt marshes. The complexity and domain expertise requirement of the process models also hamper their widespread usage as ecological engineering tools for coastal restoration and management.

In contrast, relatively simple and parsimonious empirical models of GHG fluxes can be built by leveraging the understanding of the relative environmental controls and the dominant drivers of the fluxes. Previous research presented regression-based empirical models mainly to explain the correlations of GHG fluxes with soil, climate, and hydrologic variables (e.g., Frolking & Crill, 1994; Roulet et al., 1992; Schedlbauer et al., 2012; Yurova et al., 2007; Yvon-Durocher et al., 2014). Estimated parameters of these empirical models were tailored to be site- and/or time-specific, hindering their transferability across climatic and biogeochemical gradients. Further, these empirical models were mostly developed for freshwater (tidal and nontidal) wetlands. Since salinity significantly influences the CO_2 uptake of wetland plants, as well as soil biogeochemistry and CH_4 fluxes, the freshwater models cannot be directly applied as predictive tools for coastal salt marshes.

Scaling provides critical insights into the structural and functional relationships of environmental processes with the major drivers by facilitating information transfer across different temporal and spatial domains (Blöschl & Sivapalan, 1995; Sposito, 2008). Successful scaling can, therefore, lead to the development of generalized (scale invariant) predictive models for an environmental system (Ishtiaq & Abdul-Aziz, 2017). The concept of similarity-based emergent scaling has been explored for robust predictions in various biological and environmental sciences (e.g., Enquist et al., 2003; Hondzo et al., 2013; Schwefel et al., 2017; Warnaars et al., 2007). A well-known example of emergent scaling in biology is the power law ($f(x) = ax^b$; a = constant, b = exponent) based "Kleiber's law," which states that a plant's metabolic rate increases with the body mass with an exponent of 0.75 (Savage et al., 2004). Power law relationships can represent a unique "scale invariance" or "scale-free" attribute; that is, the functional relations do not change when the magnitude (scale) of the driving variable is altered (Farrior et al., 2016; Guan et al., 2016; Serran et al., 2018; Serran & Creed, 2016). Enquist et al. (2003) leveraged Kleiber's law to develop a generalized empirical model of nightly respiration fluxes as a function of inverse temperature for various terrestrial ecosystems across the United States and Europe.

The main objective of this paper is to determine the environmental controls and emergent scaling of the major GHG fluxes of CO_2 and CH_4 in coastal salt marshes. The underlying hypothesis is that the salt marsh GHG fluxes represent emergent scaling relationships with their environmental drivers, leading to parsimonious predictive models. The research was conducted by collecting field data from four salt marshes on southern Cape Cod (Waquoit Bay and adjacent estuaries), MA, incorporating a range of nutrient loading conditions. The relative controls of various environmental drivers on the salt marsh GHG fluxes are first investigated and estimated by employing a systematic data analytics methodology (Ishtiaq & Abdul-Aziz, 2015). Dominant drivers of the fluxes are identified by resolving their mutual correlations in the multivariate space alongside process understanding. Data for the dominant drivers are then leveraged to develop simple, parsimonious, and emergent power law-based scaling models to predict the salt marsh GHG fluxes from a small set of dominant environmental drivers. The empirical scaling models are represented in a user-friendly Excel spreadsheet named "Coastal Wetland GHG Model" (CWGM) as an ecological engineering tool to explore scenarios of GHG fluxes in tidal marshes under a changing climate and environment.

2. Materials and Methods

2.1. Study Area

The study area represents the coastal salt marshes located on the shore of the North Atlantic Ocean at Cape Cod, Massachusetts. The marsh system includes several subembayments, incorporating a range of human population density and a large gradient (up to 50-fold difference) of nitrogen (N) load per unit area of estuary (Kroeger et al., 2006; Valiela et al., 2000). Four salt marshes representing a range of nutrient loading were selected for the study (Figure 1): (i) Sage Lot Pond (SL), (ii) Eel Pond (EP), (iii) Great Pond (GP), and (iv) Hamblin Pond (HP). All the study sites except for Great Pond are located inside Waquoit Bay (MA), which encompasses approximately 121.5 ha of public and privately owned salt marshes (Waquoit Bay National Estuarine Research Reserve, 2014). SL represents relatively low N loading conditions (~5 $kg \cdot ha^{-1} \cdot year^{-1}$); HP represents low to medium N loading (~29 $kg \cdot ha^{-1} \cdot year^{-1}$), whereas EP (~63 $kg \cdot ha^{-1} \cdot year^{-1}$) and GP (~126 $kg \cdot ha^{-1} \cdot year^{-1}$) represent medium to high N loading. The N loading rates reflected existing estimates, which were obtained by extensive sampling and measurement of total dissolved N concentrations in groundwater, as well as by load calculations based on annual water budgets for each watershed and application of a land use-based nitrogen loading model (Cole et al., 2005; Valiela et al., 2000).

The four wetlands are characterized by moderate to high salinity (mesohaline to polyhaline), tidal flooding, and native *Spartina alterniflora* (C_4 plant)-dominated vegetation community in the low marsh zone. Based on tide data at the nearby Woods Hole, MA station (ID: 8447930; National Oceanic and Atmospheric Administration [NOAA], 2017), the study region is subject to semidiurnal tides, representing a mean sea level (MSL) of −3.3 cm during 2013 and −5.9 cm during 1996–2013, relative to NAVD 88. The mean tidal range was 54.9 cm during 2013 and 54.3 cm during 1996–2013, indicating a microtidal (<200 cm) regime (Davies, 1964). The MSL increased since 1930 at an estimated linear rate of 0.28 cm/year.

2.2. Data Collections and Processing

The NEE of CO_2 and CH_4, as well as the environmental variables (PAR, air and soil temperatures, water level, soil moisture, and porewater salinity and pH) were measured for different days during May–October (extended growing season) of 2013 across the four salt marshes. The variables represent potential drivers and processes components (e.g., climate, hydrology, and soil biogeochemistry) of the CO_2 and CH_4 fluxes. At least three plots were established within 6.5 m^2 area in the low marsh at each site (three plots in both SL and GP and four plots in both HP and EP). Additionally, each of the three plots at the relatively pristine site (SL) had three subplots (56 cm × 56 cm), which were spaced at least 12 m and no farther than 50 m apart. Instantaneous measurements of fluxes and environmental variables were made in 20 plots to incorporate diurnal variability and tidal (low versus high) regimes between 8 a.m. and 8 p.m. The marshes were inundated during high tides and remained mostly saturated during low tides.

The NEE of CO_2 and CH_4 were measured with a cavity ring-down spectrometer gas analyzer (Model G2301, Picarro, Inc., Santa Clara, CA; frequency: 1 Hz; precision level: 0.4 ppm for CO_2 and 3 ppb for CH_4). Tubing connected the cavity ring-down spectrometer analyzer to a transparent, closed acrylic chamber (60 cm × 60 cm × 60 cm), which was sequentially placed on top of the plots in the marshes. The collars

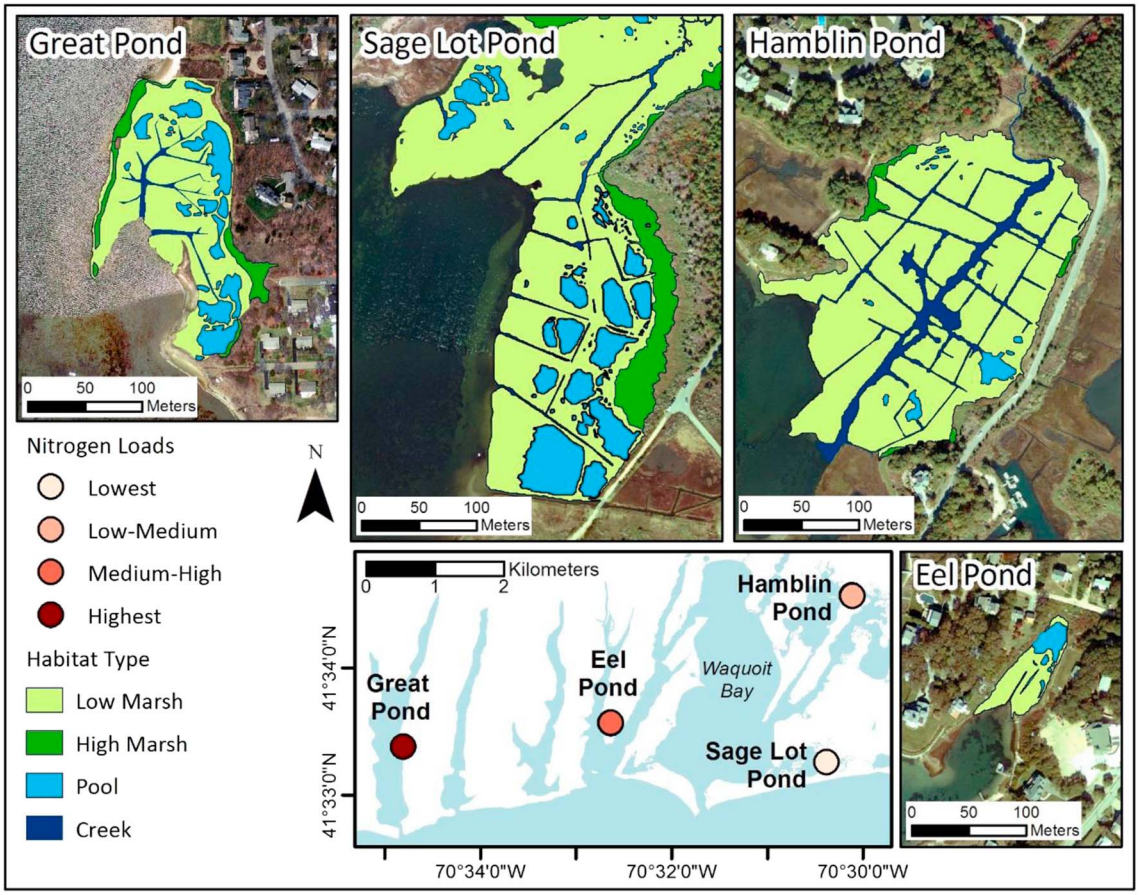

Figure 1. Locations of the four salt marshes in the Waquoit Bay and adjacent estuaries, MA. The nitrogen loading rates were approximately 5, 29, 63, and 126 $kg \cdot ha^{-1} \cdot year^{-1}$ at the Sage Lot Pond, Hamblin Pond, Eel Pond, and Great Pond sites, respectively.

were permanently installed in each plot to minimize any disturbance from chamber placement. The measured CO_2 fluxes represented both daytime net uptake ($NEE_{CO2,uptake}$) and evening/nighttime (henceforth "nighttime") net respiration ($NEE_{CO2,emission}$). $NEE_{CO2,uptake}$ were obtained during 8 a.m. to 4:30 p.m. (Eastern Standard Time, EST), whereas $NEE_{CO2,emission}$ were obtained at or after sunset between 4:30 p.m. and 8 p.m. EST ($PAR \leq 1.5\ \mu mol \cdot m^{-2} \cdot s^{-1}$). However, all measured CH_4 fluxes represented net emissions ($NEE_{CH4,emission}$) from the salt marshes. We used the notation, NEE to refer to the exchanges of CO_2 or CH_4 to be consistent among the three instantaneous fluxes. The negative and positive values of NEE conventionally indicated the net uptake and emission of GHG, respectively.

The molar concentrations of each GHG were calculated with the ideal gas law using the field measured air temperature (AT) and atmospheric pressure. Chamber artifacts were minimized by utilizing short deployment times (5–10 min), and the air inside the chambers was circulated using battery-powered fans. Fluxes were calculated by linearly regressing instantaneous GHG concentrations with time (second, s) and normalizing the regression slopes (i.e., rate of change in molar concentrations) by the chamber area (60 cm × 60 cm) for each sampling period (typically ~5 min). AT was therefore excluded from the data sets for further analysis to avoid spurious correlation with the fluxes. Instead, ST was considered to represent the impact of temperature on fluxes. ST was measured at a depth of 5 cm using an Onset U23-004 HOBO Pro v2 External Temperature Data Logger every 10 s for the duration of chamber deployments; the measurements were averaged to obtain a single value of ST over each sampling period of fluxes.

PAR was measured on-site by using a smart sensor (Onset Computer Corporation, Model # S-LIA-M003) at the time of flux sampling. Soil moisture content (SM) was measured inside the flux measurement plots with a Decagon Electrical Conductivity-5 (EC-5) sensor at a depth of 5 cm. The corresponding porewater salinity

Table 1
Summary of the Relative Linkage Data Sets for GHG Fluxes and Environmental Variables During June–October 2013 at Four Salt Marshes in Waquoit Bay and Adjacent Estuaries, MA

Data set	Variables	Mean	Standard deviation	Minimum	Maximum
Net uptake fluxes of CO_2; sample size, $N = 73$	$NEE_{CO2,uptake}$ ($\mu mol \cdot m^{-2} \cdot s^{-1}$)	−7.17	5.03	−0.05	−17.10
	PAR ($\mu mol \cdot m^{-2} \cdot s^{-1}$)	1,468.80	527.35	303.70	2,080.37
	ST (°C)	19.11	4.56	8.89	26.10
	SS (ppt)	29.53	4.00	20.00	36.00
	pH	6.80	0.34	6.05	7.87
	h (m)	0.46	0.06	0.36	0.64
	SM (%)	63.89	3.32	51.20	68.67
Net emission fluxes of CH_4; sample size, $N = 63$	$NEE_{CH4,emission}$ ($nmol \cdot m^{-2} \cdot s^{-1}$)	1.15	0.72	0.10	2.83
	PAR ($\mu mol \cdot m^{-2} \cdot s^{-1}$)	1,342.15	673.55	115.58	2,080.37
	ST (°C)	20.25	4.05	8.89	26.35
	SS (ppt)	29.10	3.81	20.00	34.00
	pH	6.88	0.31	6.30	7.87
	h (m)	0.45	0.10	0.13	0.64
	SM (%)	63.66	3.58	51.20	68.67

Note. $NEE_{CO2,uptake}$, $NEE_{CH4,emission}$, PAR, ST, SS, pH, *h*, and SM refer to the daytime net uptake fluxes of CO_2, net emission fluxes of CH_4, photosynthetically active radiation, soil temperature, porewater salinity, pH, well water level, and soil moisture content, respectively; ppt refers to parts per thousand. The negative sign indicates the net uptake fluxes of CO_2; *h* represents the water level relative to the base of wells inserted at 40 cm depth from the ground surface of the marshes.

(SS) was measured with a handheld refractometer by squeezing drops of water extracted from approximately 5 ml of surface soil. pH was measured with a surface probe pH meter (Extech Instruments, Nashua, NH). Water level sensors were placed within a 50-cm tall well at each of the four salt marshes; 40 cm of each well was driven vertically into the soil and screened with a mesh size of 0.5 mm. Well water level (h), relative to the base of the well, was recorded using a nonvented automated pressure transducer and was corrected for barometric pressure post hoc (water level logger: Onset Computer Corporation, Model #U20-001-02-TI; barometric pressure sensor: Vaisala PTB101B Barometer, WBNERR meteorological station).

The data set was subsampled by excluding the instantaneous data panels that had missing values for one or multiple environmental variables associated with the GHG fluxes. We then applied a two-step filtering procedure to ensure the QA/QC of measurements. The first filtering step was based on the coefficient of determination (R^2) of the linear regression used to convert GHG concentration to flux. A threshold R^2 of 0.90 and 0.80 were set for NEE_{CO2} and NEE_{CH4}, respectively (Moseman-Valtierra et al., 2016). Any flux observation below the respective threshold was removed from the data matrix along with the corresponding environmental drivers. The second filtering step included removal of outliers by applying the interquartile range (IQR) criteria (Tukey, 1977). Observations outside the ranges of Q1 − 1.5*IQR and Q3 + 1.5*IQR (Q1 = first quartile, Q3 = third quartile, and IQR = Q3 − Q1) for individual variables were removed along with other co-measured variables.

Analysis of the relative environmental linkages and controls required availability of data for GHG fluxes and all selected environmental variables. However, all sampling days in May and some sampling days during June–October did not have measurements for all environmental variables, and were therefore excluded from the linkage analyses. The two-step filtering led to the exclusion of 19% and 17% of observations from the primary linkage data sets of $NEE_{CO2,uptake}$ and $NEE_{CH4,emission}$, respectively. Combining four marshes, the final data sets for determining the relative linkages of fluxes with the environmental variables included 73 and 63 observation panels for $NEE_{CO2,uptake}$ and $NEE_{CH4,emission}$, respectively (Table 1). The linkage data set for $NEE_{CO2,uptake}$ had multiple observations representing 14 days during June to October: 4 days in June, 2 days in July, 4 days in August, 2 days in September, and 2 days in October. The linkage data set for $NEE_{CH4,emission}$ had meaningful observations for 12 days: 4 days in June, 1 day in July, 4 days in August, 1 day in September, and 2 days in October. The filtered flux and environmental variables varied across the four tidal marshes (Tables S1 and S2 in the supporting information). Subject to the lack of adequate measurements, a detailed investigation into the relative environmental controls of the nighttime respiration fluxes of CO_2 ($NEE_{CO2,emission}$) was not possible. Instead, based on available data and existing literature (Lloyd & Taylor, 1994; Mahecha et al., 2010; Tong et al., 2014; Xie et al., 2014), ST was considered the main driver and sole predictor of $NEE_{CO2,emission}$ in this research.

The predictive modeling data sets for $NEE_{CO2,uptake}$ and $NEE_{CH4,emission}$ were prepared once the major drivers of the individual fluxes were identified by the data analytics approaches (see section 3.6 for details). Availability of additional data for the reduced set of variables allowed an expansion of the predictive modeling data sets over May to October for both $NEE_{CO2,uptake}$ and $NEE_{CH4,emission}$. However, the two-step filtering led to the exclusion of 12% and 25% of observations from the primary modeling data sets of $NEE_{CO2,uptake}$ and $NEE_{CH4,emission}$, respectively. Combining the four marshes, the net CO_2 uptake data set included 5 days in May, 6 days in June, 1 day in July, 4 days in August, 4 days in September, and 5 days in October; the net CH_4 emission data set included the same sampling days with one additional day in May. The predictive modeling data set for ST versus $NEE_{CO2,emission}$ had measurements for 8 days: 2 days in May, 2 days in June, 1 day in July, 1 day in August, and 2 days in October. The sample size for the predictive modeling data sets was 137, 22, and 107 for $NEE_{CO2,uptake}$, $NEE_{CO2,emission}$, and $NEE_{CH4,emission}$, respectively (see details in Table S3 in the supporting information). The final data sets represented a considerable variation in GHG fluxes across the growing season days and diurnal hours (Figures S1 and S2 in the supporting information). The SL, HP, GP, and EP sites, respectively, represented 51%, 14%, 19%, and 16% of the CO_2 flux data; the corresponding site representations of CH_4 flux data were 52%, 16%, 12%, and 20%, respectively. We pooled the full set of data from all four marshes to incorporate a range of nutrient loadings and other environmental drivers, and estimate emergent scaling-based generalized predictive models of GHG fluxes for Waquoit Bay and adjacent areas.

2.3. Analysis of Variance to Compare the GHG Fluxes Across Four Salt Marshes and Tidal Conditions

One-way analysis of variance (ANOVA) was used to test the null hypothesis that there were no significant differences in GHG fluxes ($NEE_{CO2,uptake}$ and $NEE_{CH4,emission}$) with the nitrogen loading gradient (5–126 kg $N \cdot ha^{-1} \cdot year^{-1}$) among the four salt marshes. One-way ANOVA was also used to examine the effect of tidal conditions (low versus high tides) on the measured fluxes across the four salt marshes. The ANOVA analyses were conducted using the predictive modeling data sets (Table S3 in the supporting information) because of their larger sample sizes than that of the relative linkage data sets. Data were $\log_{10}$ transformed prior to the analysis to incorporate the inherent nonlinearity and achieve an approximate normal distribution in the observed GHG fluxes.

2.4. Data Analytics to Determine the Relative Environmental Controls of GHG Fluxes

A systematic data analytics methodology (Ishtiaq & Abdul-Aziz, 2015) was utilized to estimate the relative environmental controls and dominant drivers of $NEE_{CO2,uptake}$ and $NEE_{CH4,emission}$ in the coastal marshes. The analytics involved a sequential application and synthesis of Pearson correlation analysis, principal component analysis (PCA) and factor analysis (FA) (Jolliffe, 1993), and partial least squares regression (PLSR) modeling (Wold et al., 2001). Data for all variables were $\log_{10}$ transformed to incorporate any nonlinear process interactions, and then standardized by calculating their Z-scores (dimensionless) to bring different variables and units onto a comparable scale as follows: $Z = \frac{X - \overline{X}}{s_X}$, where X = $\log_{10}$-transformed variable, $\overline{X}$ = average of X, and S_X = standard deviation (SD) of X. Absolute values of the negative fluxes ($NEE_{CO2,uptake}$) were considered for analysis and modeling in the nonlinear ($\log_{10}$) domain.

The correlation analysis provides important background information on the correspondences between the GHG fluxes and their predictors. However, the correlation coefficients are inherently inconclusive and could be misleading subject to the impact of multicollinearity (mutual correlations) among the driving variables. Both PCA and FA resolve multicollinearity by using orthogonal projections to mine the underlying interrelations and linkage patterns among the flux and the driving variables. However, the mechanisms of PCA and FA are different, although none involves a direct estimation of the predictors versus response relationship. In this study, PCA was conducted by deriving orthogonal (independent) entities called principal components (PCs; as many as the number of original variables), where each PC was a linear combination of all original (response and predictor) variables. In contrast, FA was conducted by decomposing all original (response and predictor) variables into a smaller set of latent entities called factors. The important latent factors were extracted based on an eigenvalue criterion (eigenvalue $\geq$ 1.0) for a maximum explanation of data system variance with fewer factors. Further, the "varimax" rotation was performed to optimize the loadings of the original variables on

each factor. The synthesis of PCA and FA provided a confirmatory understanding of the interrelation and linkage patterns among the GHG fluxes and the environmental drivers.

PLSR models were developed to directly estimate the individual controls of the drivers on GHG fluxes. We did not employ a conventional principal component regression (PCR), because the PCs for a PCR are first computed by decomposing only the predictors (unlike the PCA in this study) and then fitted with the response in two separate steps, which does not ensure an optimal explanation of variance in the response (Jolliffe, 1993). However, the partial least squares (PLS) components in PLSR are computed and maximally linked with the response variable by a simultaneous decomposition of the response and all predictors (Schumann et al., 2013). The PLSR modeling resolves multicollinearity to avoid spurious correlations in the data matrix. This is achieved by fitting models in the orthogonal domain with a minimum number of PLS components as predictors (Kuhn & Johnson, 2013; Wold et al., 2001). The most accurate and consistent models of fluxes were identified based on a synthesis of the minimum Akaike Information Criterion (AIC) (Akaike, 1974) and the maximum Nash-Sutcliffe Efficiency (NSE; Text S1 in the supporting information). The PLSR model parameters were robustly estimated using the SIMPLS algorithm (de Jong, 1993) and a 10-fold cross-validation (Kuhn & Johnson, 2013).

Estimated parameters of the PLSR models were converted back to the *Z*-score domain of the original variables to quantify the relative controls (weights, β) of the individual environmental drivers on the GHG fluxes. The weights of individual drivers were aggregated to compute the strength of linkages between GHG fluxes and the "climatic" (β_C; including PAR and ST), "biogeochemical" (β_B; SS and pH), and "hydrologic" (β_H; *h* and SM) process components using the method of vector summation as follows:

$$\beta_C = \sqrt{\beta_{PAR}^2 + \beta_{ST}^2} \tag{1}$$

$$\beta_B = \sqrt{\beta_{SS}^2 + \beta_{pH}^2} \tag{2}$$

$$\beta_H = \sqrt{\beta_h^2 + \beta_{SM}^2} \tag{3}$$

Although the variables within a process component may be interlinked, the aggregated linkages of the components are relatively unbiased given that the individual variable weight (β) were estimated with PLSR by appropriately resolving multicollinearity. The relative linkages of different process components with the GHG fluxes were compared to the "climatic" component by calculating the ratios of β_C/β_B and β_C/β_H. Results of the four-layer data analytics were synthesized to characterize the relative controls of environmental drivers on $NEE_{CO2,uptake}$ and $NEE_{CH4,emission}$, and identify their dominant predictors.

2.5. Predictive Modeling of GHG Fluxes With Emergent Scaling Functions

Emergent power law scaling-based predictive models of the salt marsh GHG fluxes were developed as a function of the dominant and mechanistically meaningful predictors using the original data (i.e., without centralization and normalization to *Z*-scores) as follows:

$$NEE_{GHG} = 10^a X_1^{b_1} X_2^{b_2} X_3^{b_3} \ldots X_k^{b_k} \tag{4}$$

where NEE_{GHG} = net fluxes of CO_2 or CH_4 (i.e., $NEE_{CO2,uptake}$, $NEE_{CO2,emission}$, or $NEE_{CH4,emission}$), k = number of dominant predictors, a and b_k = model parameters (i = 1, 2, …, k), and X_k = environmental predictors. The parameters b_k represent the exponents of the emergent power law scaling relationships between a GHG flux variable and the major environmental predictors. The power law scaling models were built in a parsimonious way by involving the smallest set of dominant predictors, which had been identified through data analytics (details in section 3.6). The models were estimated numerically with data using the Levenberg-Marquardt least squares technique (a variant of Gauss-Newton algorithm; Seber & Wild, 2003, 2005) in MATLAB. The modeling data sets were replicated 10,000 times (i.e., total number of observations = original sample size × 10,000) using bootstrap resampling to achieve 10,000 model estimations. A cross-validation algorithm was also incorporated into the model estimation framework to further a robust estimation of parameters. In each iteration, 80% of the data were used for model calibration (training) and the remaining 20% were used for validation (independent testing). The averages of 10,000 estimated values for individual parameters were

Table 2
Pearson Correlation Matrix for the Net Uptake Fluxes of CO_2 and Net Emission Fluxes of CH_4 With the Environmental Variables at Four Salt Marshes in Waquoit Bay and Adjacent Estuaries, MA

Variable	PAR	ST	SS	pH	*h*	SM	NEE
			Net uptake fluxes of CO_2 ($NEE_{CO2,uptake}$)				
PAR	1.00	**0.41**	**−0.38**	0.03	−0.23	0.12	**0.73**
ST	**0.41**	1.00	**−0.39**	0.08	0.03	0.05	**0.87**
SS	**−0.38**	**−0.39**	1.00	**−0.35**	−0.08	0.00	**−0.55**
pH	0.03	0.08	**−0.35**	1.00	**0.30**	−0.01	0.09
h	−0.23	0.03	−0.08	**0.30**	1.00	0.11	−0.11
SM	0.12	0.05	0.00	−0.01	0.11	1.00	0.06
NEE	**0.73**	**0.87**	**−0.55**	0.09	−0.11	0.06	1.00
			Net emission fluxes of CH_4 ($NEE_{CH4,emission}$)				
PAR	1.00	**0.47**	**−0.45**	0.03	0.09	0.04	**0.63**
ST	**0.47**	1.00	−0.21	−0.08	−0.25	0.04	**0.81**
SS	**−0.45**	−0.21	1.00	**−0.29**	−0.10	0.01	**−0.38**
pH	0.03	−0.08	**−0.29**	1.00	**−0.29**	−0.01	−0.03
h	0.09	−0.25	−0.10	**−0.29**	1.00	−0.09	−0.14
SM	0.04	0.04	0.01	−0.01	−0.09	1.00	0.00
NEE	**0.63**	**0.81**	**−0.38**	−0.03	−0.14	0.00	1.00

Note. Bold indicates significant correlations at the 95% level of confidence (p value < 0.05). $NEE_{CO2,uptake}$, $NEE_{CH4,emission}$, PAR, ST, SS, pH, *h*, and SM refer to the daytime net uptake fluxes of CO_2, net emission fluxes of CH_4, photosynthetically active radiation, soil temperature, porewater salinity, pH, well water level, and soil moisture content, respectively.

used as the final parameter set to predict GHG fluxes in the tidal salt marshes. The model goodness-of-fit was measured by NSE, whereas the model accuracy was assessed by the ratio of root-mean-square error to the standard deviations of the observations (RSR; Text S1 in the supporting information). Similar to R^2, NSE = 1.0 refers to a perfect model (i.e., values closer to 1.0 indicate a better model); NSE < 0 refers to a model that is a worse predictor than the average of flux observations as an alternative model. In contrast, an RSR value of less than 0.50 indicates a highly accurate model (see Text S1 for details).

3. Results

3.1. Comparison of the GHG Fluxes Across the Salt Marshes and Tidal Conditions

Based on the one-way ANOVA, we could not reject the null hypothesis of no significant differences in $NEE_{CO2,uptake}$ ($F_{3,133} = 0.46$; p value = 0.71) or in $NEE_{CH4,emission}$ ($F_{3,103} = 0.98$; p value = 0.41) with the nitrogen loading gradient (5–126 $kg \cdot ha^{-1} \cdot year^{-1}$) among the four salt marshes at the 95% level of confidence (Table S4 in the supporting information). However, the null hypothesis of no significant difference was rejected for both $NEE_{CO2,uptake}$ ($F_{1,135} = 11.33$; p value < 0.001) and $NEE_{CH4,emission}$ ($F_{1,105} = 22.47$; p value < 0.001) at the 95% level of confidence when the respective fluxes were compared between the high tide and low tide conditions (Table S5 in the supporting information). The higher GHG fluxes corresponded to the high tides, whereas the GHG fluxes were relatively low during the low tides (Figure S3 in the supporting information).

3.2. Correlations of the GHG Fluxes and Environmental Variables

The nonlinear correlation coefficients (obtained from the $\log_{10}$-transformed and standardized data) provided first-order information about the influence of each environmental driver on the GHG fluxes (Table 2). Significance of the correlations was evaluated at the 95% level of confidence (p value < 0.05). The net uptake fluxes of CO_2 and emission fluxes of CH_4 had significant correlations with light (PAR), ST, and SS. $NEE_{CO2,uptake}$ was highly correlated with ST ($r = 0.87$) and moderately to highly correlated with PAR ($r = 0.73$). The correlation between $NEE_{CO2,uptake}$ and SS was moderately strong ($r = -0.55$). Similarly, $NEE_{CH4,emission}$ had a high correlation with ST ($r = 0.81$), a moderate to high correlation with PAR ($r = 0.63$), and a moderate correlation with SS ($r = -0.38$; Table 2). However, well water level (h), soil moisture (SM), and porewater pH were weakly and insignificantly correlated (p value > 0.05) with both fluxes. Further, significant correlations between PAR

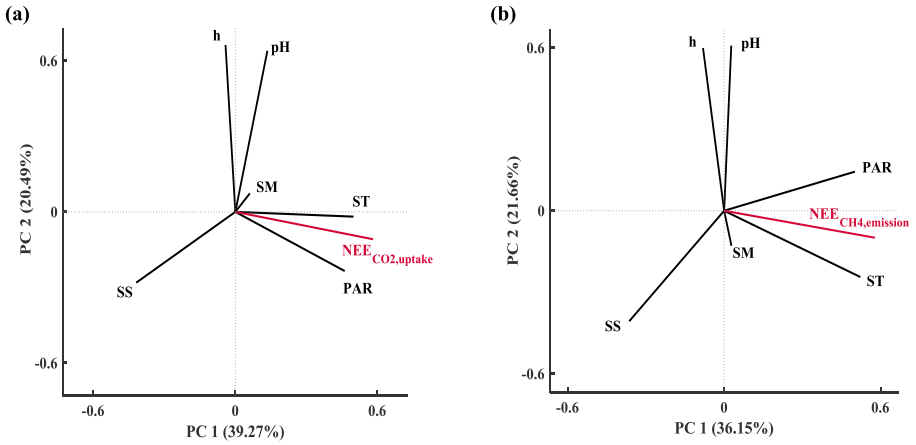

Figure 2. Biplots from principal component analysis, showing the interrelations and relative orientations of environmental variables with (a) $NEE_{CO2,uptake}$ and (b) $NEE_{CH4,emission}$ for the four salt marshes in Waquoit Bay and adjacent estuaries, MA. $NEE_{CO2,uptake}$, $NEE_{CH4,emission}$, PAR, ST, SS, pH, *h*, and SM refer to the daytime net uptake fluxes of CO_2, net emission fluxes of CH_4, photosynthetically active radiation, soil temperature, porewater salinity, pH, well water level, and soil moisture content, respectively. PC = principal component.

and ST (r = 0.41 to 0.47), SS and ST (r = −0.21 to −0.39), and SS and pH (r = −0.29 to −0.35) were apparent—indicating the presence of a considerable multicollinearity among the environmental drivers.

3.3. Relative Orientations and Controls of the Environmental Drivers on GHG Fluxes

The PCA loadings obtained from the first two PCs for $NEE_{CO2,uptake}$ and $NEE_{CH4,emission}$ were presented through biplots, where PC1 and PC2 explained 36–39% and 20–22% of the data variance, respectively (Figure 2). The two fluxes loaded highly on the first PC and relatively weakly on the second PC. The strong loadings of PAR and ST on PC1, as well as their distinctly non-orthogonal orientations, indicated their high interrelationships and strong positive controls on the fluxes. Moderate loadings of the SS vector on both PCs and its direction along PC1 suggested moderate negative linkages of porewater salinity with both fluxes. In contrast, well water level (h) and pH loaded very weakly on PC1 and strongly on PC2—indicating their weak controls on both $NEE_{CO2,uptake}$ and $NEE_{CH4,emission}$. However, the fluxes had the weakest linkages with SM, as apparent in its very small loadings on both PCs.

3.4. Dominant Environmental Factors and Drivers of the GHG Fluxes

Three orthogonal latent factors were extracted based on the eigenvalue ≥ 1 criterion for both $NEE_{CO2,uptake}$ and $NEE_{CH4,emission}$ (Table 3). The three factors together explained approximately 60% of the respective data

Table 3
Dominant Factors and Optimized Loadings of the Fluxes and the Environmental Variables for the Four Salt Marshes in Waquoit Bay and Adjacent Estuaries, MA

Net uptake fluxes of CO_2				Net emission fluxes of CH_4			
Variable	Factor 1	Factor 2	Factor 3	Variable	Factor 1	Factor 2	Factor 3
PAR	0.37	**0.78**	0.02	PAR	**0.49**	0.02	**0.65**
ST	**1.00**	0.05	0.05	ST	**0.93**	−0.05	0.02
SS	−0.35	−0.36	**−0.55**	SS	−0.24	−0.28	**−0.50**
pH	0.05	−0.04	**0.64**	pH	−0.03	**1.00**	0.04
h	0.03	−0.34	0.39	*h*	−0.26	0.26	0.28
SM	0.04	0.04	0.00	SM	0.03	−0.01	−0.02
$NEE_{CO2,uptake}$	**0.84**	**0.52**	0.11	$NEE_{CH4,emission}$	**0.86**	−0.01	0.32

Note. Bold values indicate dominant loadings on each factor. $NEE_{CO2,uptake}$, $NEE_{CH4,emission}$, PAR, ST, SS, pH, *h*, and SM refer to the daytime net uptake fluxes of CO_2, net emission fluxes of CH_4, photosynthetically active radiation, soil temperature, porewater salinity, pH, well water level, and soil moisture content, respectively.

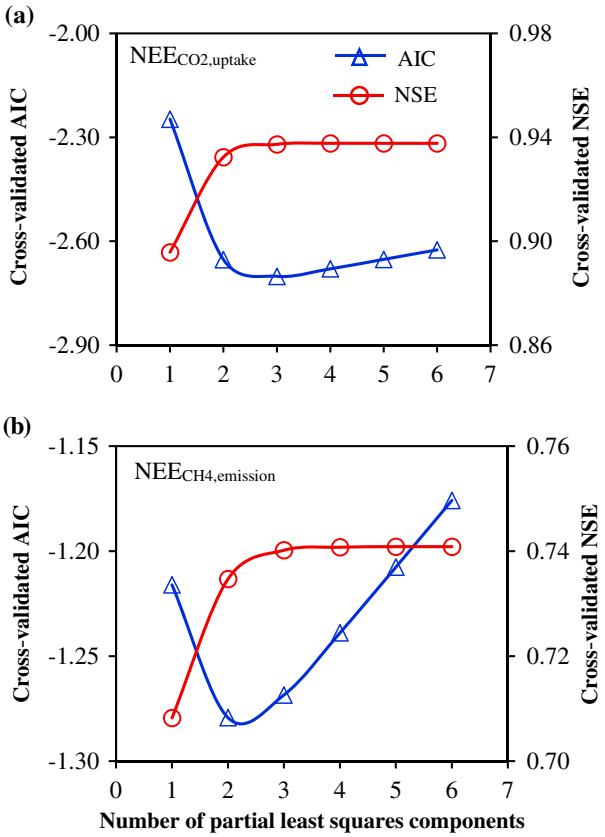

Figure 3. Plots of cross-validated (a) normalized Akaike Information Criterion (AIC) and (b) Nash-Sutcliffe Efficiency (NSE) for the greenhouse gas fluxes with the number of partial least squares components.

variance for the GHG fluxes. Both fluxes had their high loadings (0.84 and 0.86, respectively) on factor 1. The high loadings (0.93 to 1.00) of ST on factor 1 suggested strong linkages of the fluxes with the ambient ST. $NEE_{CO2,uptake}$ and PAR, respectively, had a moderate (0.52) and a high (0.78) loading on factor 2, indicating the control of sunlight on the daytime net CO_2 uptake. In contrast, the weak to moderate loading of $NEE_{CH4,emission}$ (0.32) and the moderate to high loading of PAR (0.65) on factor 3 suggested a moderate linkage of sunlight with the methane emission fluxes. However, the moderate loading of PAR (0.49) on factor 1—where both $NEE_{CH4,emission}$ and ST loaded highly—indicated the potential impact of mutual linkage between PAR and temperature on the explanation of variance in the methane fluxes. SS loaded moderately (−0.50 to −0.55) on factor 3 and weakly to moderately (−0.24 to −0.36) on factors 1 and 2, referring to a noteworthy linkage of soil porewater salinity with both fluxes. Although pH loaded highly (1.00) on factor 2 for $NEE_{CH4,emission}$ and moderate to highly (0.64) on factor 3 for $NEE_{CO2,uptake}$, the small loadings of fluxes on the respective factors suggested their weak linkages with pH (Table 3). The hydrology variables (h and SM) did not have dominant loadings on any factor—suggesting their weak controls on the fluxes for these moderate to highly saline coastal marshes (Table 1).

3.5. Estimations of the Environmental Controls of GHG Fluxes With PLSR

The nonlinear PLSR models (with the *Z*-score data) directly estimated the relative controls of the environmental variables on the GHG fluxes. The cross-validated minimum AIC and maximum NSE criterion led to the inclusion of 2–3 PLS components to obtain the optimal PLSR models (Figure 3). The explanatory models of $NEE_{CO2,uptake}$ and $NEE_{CH4,emission}$ were statistically significant (F statistic = 47–289, p value < 0.0001), exhibiting a good fitting efficiency and accuracy (NSE = 0.73–0.94, RSR = 0.25–0.51; Table 4). ST was the most influential (highest weight) variable in regression—exhibiting approximately 2, 4–5, 8–16, 12–22, and 15–33 times stronger controls on the fluxes than that of PAR, SS, h, pH, and SM, respectively (Table 4). Based on the aggregated linkages (equations (1)–(3)), the "climatic" component (ST and PAR) had approximately 5 and 19 times stronger controls on $NEE_{CO2,uptake}$ than that of the "biogeochemical" (SS and pH) and "hydrologic" (h and SS) components, respectively. Similarly, $NEE_{CH4,emission}$ was 5 and 8 times more strongly linked with the "climatic" component than with the "biogeochemical" and "hydrologic" components, respectively.

3.6. Development of Emergent Scaling-Based Predictive Models of GHG Fluxes

The four-layer data analytics provided important insights for identifying the most dominant environmental drivers of GHG fluxes in coastal salt marshes. Based on the nonlinear correlation coefficients of the $\log_{10}$ domain, the $NEE_{CO2,uptake}$ and $NEE_{CH4,emission}$ had strong, moderate to strong, and moderate correspondences with the ST, PAR, and SS, respectively (albeit impacted by multicollinearity). PCA and FA resolved multicollinearity in two reverse but complementary orthogonal transformations. PCA suggested a strong linkage of the GHG fluxes with both ST and PAR and a moderate linkage with SS. In contrast, FA indicated a strong linkage of the fluxes with ST and a weak to moderate linkage with SS and PAR. However, both PCA and FA provided indirect measures of the nonlinear relations between fluxes and the driving variables. The direct estimations of predictors versus response relations with the orthogonal component-based nonlinear PLSR modeling suggested ST, PAR, and SS as, respectively, the strong, moderate, and weak drivers of the fluxes. Further, all four layers of analytics indicated that pH, h, and SM were not important drivers of the GHG fluxes in these coastal salt marshes.

Based on the above synthesis, PAR, ST, and SS were primarily chosen as the dominant predictors for both $NEE_{CO2,uptake}$ and $NEE_{CH4,emission}$ models. Subject to the availability of additional data for fluxes and the

Table 4
Coefficients (β) of the Log_{10}-Transformed, Standardized (Z-Score) PLSR Models for $NEE_{CO2,uptake}$ and $NEE_{CH4,emission}$ for Four Salt Marshes in Waquoit Bay and Adjacent Estuaries, MA

	$NEE_{CO2,uptake}$		$NEE_{CH4,emission}$	
Predictors	β	$\beta_{ST}/\beta_{Variable}$	β	$\beta_{ST}/\beta_{Variable}$
PAR	0.39	1.7	0.31	1.9
ST	0.65	1.0	0.60	1.0
SS	−0.16	4.1	−0.12	5.0
pH	−0.03	21.7	−0.05	12.0
h	−0.04	16.3	−0.08	7.5
SM	−0.02	32.5	−0.04	15.0
	PLSR statistics			
PLS components	3		2	
NSE	0.94		0.73	
RSR	0.25		0.51	
	Aggregated linkages			
β_C	0.76		0.68	
β_B	0.16		0.13	
β_H	0.04		0.09	
β_C/β_B	4.8		5.2	
β_C/β_H	19.0		7.6	

Note. $NEE_{CO2,uptake}$, $NEE_{CH4,emission}$, PAR, ST, SS, pH, *h*, and SM refer to the daytime net uptake fluxes of CO_2, net emission fluxes of CH_4, photosynthetically active radiation, soil temperature, porewater salinity, pH, well water level, and soil moisture content, respectively. The aggregated linkages of the "climatic" (β_C), "biogeochemical" (β_B), and "hydrologic" (β_H) process components were computed, respectively, from equations (1), (2), and (3). $\beta_{ST}/\beta_{Variable}$ represents the ratio between the coefficient of ST and the coefficients of other variables in the partial least squares regression (PLSR) model. NSE = Nash-Sutcliffe Efficiency; PLS = partial least squares; RSR = ratio of root-mean-square error to the standard deviations of the observations.

reduced set of drivers, the predictive models were then estimated with extended data sets for May to October 2013 (Table S3; details in section 2.2). The estimated parameters of all three predictors in the $NEE_{CO2,uptake}$ model were statistically significant (N = 137, p value < 0.001). However, the parameter of PAR was not statistically significant (p value = 0.54) for the $NEE_{CH4,emission}$ model. Therefore, the final model of $NEE_{CH4,emission}$ included only ST and SS as the significant, dominant predictors (N = 107, p value < 0.05). Furthermore, based on available data and the existing literature (Lloyd & Taylor, 1994; Mahecha et al., 2010; Tong et al., 2014; Xie et al., 2014), the nighttime net CO_2 respiration ($NEE_{CO2,emission}$) was modeled as a power law function of ST (N = 22, p value < 0.001).

The final models of the GHG fluxes—as robustly estimated with a bootstrap Monte-Carlo process using 10,000 iterations—showed a very good agreement with observed fluxes of the four salt marshes. The mean fitting efficiency (NSE) and prediction accuracy (RSR) of the $NEE_{CO2,uptake}$ model over 10,000 estimations (calibrations) were 0.91 and 0.31, respectively; the model performed equally well for 10,000 validations (mean NSE = 0.90, mean RSR = 0.30). The $NEE_{CO2,emission}$ model provided similar predictions in calibrations and validations (mean NSE = 0.87–0.89, mean RSR = 0.30–0.36). The $NEE_{CH4,emission}$ model also showed good performance over the 10000 calibrations (mean NSE = 0.83, mean RSR = 0.42) and validations (mean NSE = 0.80, mean RSR = 0.49). Ensemble means of the individual parameters were used to represent the final, emergent power law scaling models of the GHG fluxes as follows:

$$NEE_{CO2,uptake} = -10^{-3.99} PAR^{0.66} ST^{3.28} SS^{-1.07} \quad (5)$$

$$NEE_{CO2,emission} = 10^{-1.43} ST^{1.49} \quad (6)$$

$$NEE_{CH4,emission} = 10^{-2.61} ST^{3.45} SS^{-1.35} \quad (7)$$

where $NEE_{CO2,uptake}$, $NEE_{CO2,emission}$, and PAR represent the original (i.e., untransformed) data in $\mu mol \cdot m^{-2} \cdot s^{-1}$; $NEE_{CH4,emission}$ is in $nmol \cdot m^{-2} \cdot s^{-1}$; ST is in °C; and SS is in parts per thousand (ppt). The negative sign in equation (5) indicates the daytime net uptake fluxes of CO_2.

The observed GHG fluxes were plotted against the predicted fluxes to further demonstrate the performance and spatial robustness of the models across the four salt marshes (Figure 4). The model parameters were approximately normally distributed, as demonstrated by the sampling distribution of 10,000 estimations. Standard deviation (SD) of the $NEE_{CO2,uptake}$ model parameters representing the scale factor (−3.99), PAR (0.66), ST (3.28), and SS (−1.07) were, respectively, 0.52, 0.10, 0.19, and 0.22. The SD of the $NEE_{CO2,emission}$ model parameters representing the scale factor (−1.43) and ST (1.49) were, respectively, 0.18 and 0.15. The SD of the $NEE_{CH4,emission}$ model parameters associated with the scale factor (−2.61), ST (3.45), and SS (−1.35) were 0.79, 0.24, and 0.46, respectively. The small SDs relative to the respective means (coefficient of variation = 6–34%) indicated stability and low uncertainty of the estimated model parameters.

The developed models (equations (5)–(7)) were represented in a user-friendly, macro-based Excel spreadsheet model named "Coastal Wetland GHG Model" (CWGM) (see CWGM, 2018 to download the Excel model). We expressed the difference between net carbon (CO_2) uptake and net carbon (CO_2 and CH_4) emissions in the Excel model by a new term, *net atmospheric carbon removal* (NACR). The net ecosystem carbon balance of a wetland can be obtained by subtracting the net lateral flux from NACR. However, the net lateral fluxes between the salt marsh and the bay were not modeled in this study. A user can estimate the NACR by upscaling the predicted instantaneous fluxes of CO_2 and CH_4 over the growing period (or any user-defined period) in units of gram carbon (C) per square meter of marsh area (gC/m^2). The Excel-based model may aid the coastal stakeholders (e.g., reserve managers, restoration practitioners, and

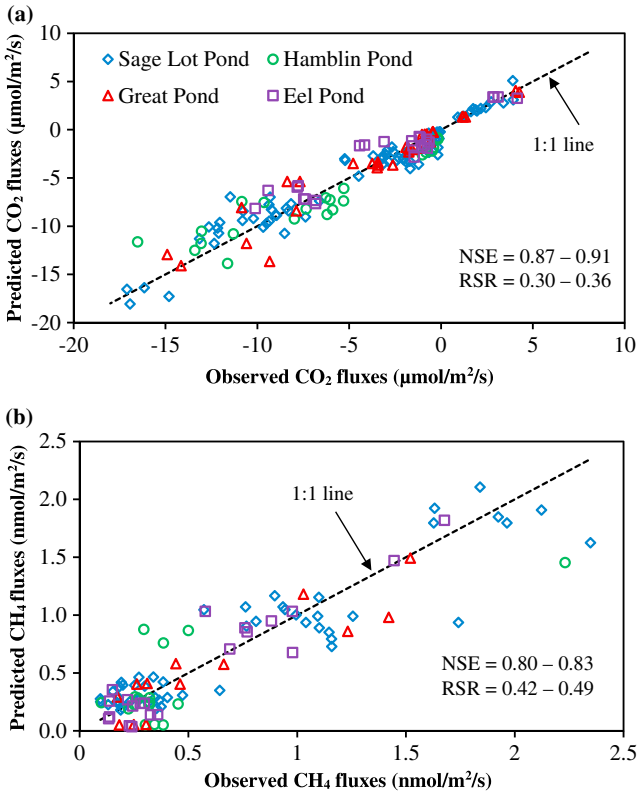

Figure 4. Observed versus predicted fluxes of (a) CO_2 ($NEE_{CO2,uptake}$ and $NEE_{CO2,emission}$) and (b) CH_4 ($NEE_{CH4,emission}$) in the four salt marshes of Waquoit Bay and adjacent estuaries, MA. Negative and positive, respectively, indicate the net uptake and emission fluxes. NSE = Nash-Sutcliffe Efficiency; RSR = ratio of root-mean-square error to the standard deviations of the observations.

policymakers) in tidal wetland monitoring and restorations, economic evaluations of blue carbon, and developing GHG offset protocols (see Text S2 in the supporting information for further details).

4. Discussion

4.1. GHG Fluxes Across the N Gradient Among the Salt Marshes

The net uptake fluxes of CO_2 and emission fluxes of CH_4 did not significantly vary across the N gradient (5–126 $kg \cdot ha^{-1} \cdot year^{-1}$) among the four salt marshes at Cape Cod, MA (Table S4); this is in contrast with previous studies on coastal salt marshes. For example, Morris et al. (2013) reported a significant increase in net primary production of *S. alterniflora* and *S. patens* in response to N fertilization of salt marshes at the rates of 1,050–2,100 $kg \cdot N \cdot ha^{-1} \cdot year^{-1}$ for 13 years at Plum Island, MA, and for 30 years at North Inlet, South Carolina. Vivanco et al. (2015) found significant increases in both net CO_2 uptake and CH_4 emission fluxes in three salt marshes (dominated by *Salicornia virginica*) across the California coasts of United States by gradually applying fertilization loads of 100–3,200 $kg \cdot N \cdot ha^{-1} \cdot year^{-1}$ over a 7–14 month period. However, Vivanco et al. (2015) reported no significant effect on CO_2 respiration by the N fertilization in the Californian marshes. We posit that the N loadings in the four marshes at Cape Cod were not high enough to result in a positive response of GHG fluxes despite the notable N gradient among them.

4.2. Environmental Controls of the Daytime Net Uptake Fluxes of CO_2

The *S. alterniflora* dominated salt marshes at Cape Cod displayed high productivity with daytime net uptake fluxes of CO_2 ($NEE_{CO2,uptake}$) in this study (mean = -7.17 $\mu mol \cdot m^{-2} \cdot s^{-1}$, SD = 5.03 $\mu mol \cdot m^{-2} \cdot s^{-1}$; Table 1). *S. alterniflora* (a C_4 plant) has a high photosynthesis rate (minimal photorespiration), compared to C_3 plants (e.g., *Phragmites australis*; Mantlana et al., 2008). *S. alterniflora* also has a well-developed aerenchyma to adapt to the hypoxic conditions of coastal wetlands (Maricle & Lee, 2007). However, fixation of CO_2 by salt marsh plants depends on the availability of sunlight (PAR), which had a moderate to high control on the net uptake fluxes of CO_2. In a companion study, Moseman-Valtierra et al. (2016) examined the variation in gas fluxes across vegetation types within the differing regions of Sage Lot Pond—reporting moderate to high linkages of CO_2 fluxes with the aboveground biomass, belowground biomass, plant height, and stem density. However, the linkage of gas fluxes with biomass or other plant variables was not tested in the present study.

The strong positive control of ST on $NEE_{CO2,uptake}$ can mainly be attributed to the accelerated photosynthesis in coastal wetlands in response to high temperature (Guo et al., 2009; Inglett et al., 2012). Ambient temperature controls the activity of the primary C_4 photosynthetic enzyme, RuBisCO. The turnover rate of RuBisCO increases with elevated temperature during the daylight hours, resulting in higher CO_2 uptake (Sage & Kubien, 2007). However, the CO_2 uptake falls at low temperatures as CO_2 leaks out from the bundle sheath cells (Kubien et al., 2003). Previous studies reported a coupled increase in photosynthesis and aboveground biomass of *Spartina* with experimental warming during the growing season (Charles & Dukes, 2009; Couto et al., 2014; Idaszkin & Bortolus, 2011). However, photosynthesis of C_4 plants can also decline or shut down at extremely high temperature (Sage, 2002; Sage & Kubien, 2007), which was not encountered during our sampling at Cape Cod in May–October 2013 (ST $<$ 30 °C; Tables 1 and S3). Further, since NEE incorporates both gross primary productivity and respiration during daytime, the estimated linkage of ST and $NEE_{CO2,uptake}$ may be different from that between ST and gross primary productivity.

Our study found a significant negative impact of soil salinity on $NEE_{CO2,uptake}$ in the *Spartina* dominated salt marshes. Although salt marsh plants are tolerant of salinity stress, marsh productivity can be adversely affected with increasing salinity (Lewis & Weber, 2002; Wang et al., 2006). Ewing et al. (1995) found

substantial decreases in the aboveground biomass of *Spartina* with salinity treatments of 14, 21, and 28 ppt over 7 to 42 days. Vasquez et al. (2006) reported a decreasing trend in both aboveground and belowground biomass of *Spartina* with increasing salinity from 0.57 to 34 ppt over a period of 3 months. High salinity affects the leaf chlorophyll content, protein synthesis, and lipid metabolism of marsh plants—resulting in overall decreased productivity (Mateos-Naranjo et al., 2010; Parida & Das, 2005; Pierfelice et al., 2015). The salinity impacts could be linked to the accumulation of phytotoxic substances (e.g., hydrogen sulfide, H_2S) in anaerobic wetland sediments (Bradley & Morris, 1990), with both salinity and phytotoxin concentrations increasing when intensity of tidal flushing is relatively low. H_2S is produced through a metabolic process in anoxic, waterlogged conditions under the influence of sulfate-reducing bacteria (e.g., *Desulfovibrio*)—with higher salinity indicating a greater supply of sulfate substrate (Lamers et al., 2013). Soil salinity and sulfide can also affect root respiration, oxygen consumption, and stomatal resistance to gas diffusion (Brown et al., 2006; Howes et al., 1986; Mendelssohn & McKee, 1988).

Porewater pH of the marsh soil was mostly at or near neutral (pH ≈ 7, Table 1), and exhibited no notable control on $NEE_{CO2,uptake}$ in the four salt marshes. $NEE_{CO2,uptake}$ was significantly higher during the high tides than the low tides in the Cape Cod salt marshes (Table S5, Figure S3). This is in agreement with other salt marsh studies (Morris, 2000; Wilson & Morris, 2012), which reported a stronger tidal flushing of accumulated salt from the marsh soil and a higher primary productivity during high tides. However, we did not find a direct predictive control of the observed modest range of well water level or soil moisture on $NEE_{CO2,uptake}$ in this analysis. The wetland soil often remained at or near complete saturation due to frequent inundation of these low marshes at Cape Cod with a semidiurnal tidal regime. Since tidal hydrology can strongly regulate the variation of ST and porewater salinity (Wang et al., 2007), it appears that the effect of hydrology on net CO_2 uptake fluxes was indirectly manifested through ST and salinity. However, it is also possible that our measured well water levels did not accurately represent the tidal fluctuations in the marsh sites due to the predominant soil saturation and an inherent time-lag between the well and tidal water levels.

4.3. Environmental Controls of the Net Emission Fluxes of CH_4

The tidal salt marshes of Cape Cod exhibited low CH_4 emissions (mean $NEE_{CH4,emission} = 1.15\ nmol \cdot m^{-2} \cdot s^{-1}$, $SD = 0.72\ nmol \cdot m^{-2} \cdot s^{-1}$; Table 1). Data analytics indicated ST as the most dominant driver of daytime CH_4 emission ($NEE_{CH4,emission}$) from the salt marshes. This is consistent globally for a range of ecosystems, including wetlands (Yvon-Durocher et al., 2014), since methanogenesis is substantially driven by temperature (Dunfield et al., 1993; Martin & Moseman-Valtierra, 2017). Further, *S. alterniflora* marshes support a composition of microbial populations (including methanogens), which could contribute to higher CH_4 emission during warmer conditions (e.g., Burke et al., 2002; Ravit et al., 2003). Microbial activity associated with both CH_4 production (methanogenesis) and oxidation (methanotrophy) is typically represented with an exponentially increasing function (e.g., Arrhenius equation) of ST and available heat energy (Walter & Heimann, 2000). However, methanogenesis can have a higher sensitivity to temperature than that of methanotrophy (Born et al., 1990; Dunfield et al., 1993), leading to higher emissions of CH_4 at elevated temperature.

The overall low emissions of CH_4 from the Cape Cod salt marshes were mainly caused by high salinity. $NEE_{CH4,emission}$ were negatively and nonlinearly related to the porewater salinity—which is consistent with existing literature on coastal wetlands (e.g., Bartlett et al., 1985, 1987; Poffenbarger et al., 2011). Previous studies (Chmura et al., 2011; Magenheimer et al., 1996; Nedwell et al., 2004; Vivanco et al., 2015) also reported low emissions of CH_4 (0.4 to 2.6 $nmol \cdot m^{-2} \cdot s^{-1}$) from moderately to highly saline (18–35 ppt) coastal wetlands. The tidal salt marsh sediments are rich in sulfate (SO_4^{2-}), which sulfate-reducing bacteria utilize as a terminal electron acceptor during anaerobic decomposition. Thermodynamically, sulfate reduction yields more energy than methanogenesis (Segers, 1998). Sulfate-reducing bacteria, therefore, outcompete methanogens, limiting CH_4 production in highly saline sulfate-rich marsh soil (Bartlett et al., 1987; Poffenbarger et al., 2011; Weston et al., 2014). In fact, SO_4^{2-} reduction can sometimes represent most of the total anaerobic decomposition in salt marsh sediments due to high SO_4^{2-} concentrations and scarcity of other terminal electron acceptors (Howarth, 1993; Weston et al., 2014). Further, CH_4 oxidation by SO_4^{2-} reducers can also reduce CH_4 emission to the atmosphere in highly saline coastal wetlands (Bartlett et al., 1987; Segers, 1998).

The methane emission fluxes at the four salt marshes did not have a notable linkage with soil porewater pH, which generally represented neutral conditions (Table 1). Subject to the high salinity and near-saturated soil

moisture conditions, our results did not show a direct predictive control of well water level or soil moisture on the salt marsh CH_4 emissions. However, the CH_4 fluxes were significantly higher during the high tides than that of the low tides (Table S5, Figure S3), indicating the stronger tidal flushing of accumulated salt in marsh soil during high tides (Morris, 2000; Wilson & Morris, 2012). Recurrent tidal flooding regulates the temporal variation of porewater salinity (Silvestri & Marani, 2004; Wang et al., 2007), ultimately impacting CH_4 production and emission in the salt marshes. The findings also suggest that any direct influence of the hydrologic variables on CH_4 fluxes likely diminishes above a certain salinity threshold (e.g., 18 ppt; see Poffenbarger et al., 2011). The intertwined effects of tide and salinity in salt marshes indicate the potential for substantially lower emissions of CH_4 if tidal flow is restored in coastal wetlands to increase salinity above 18 ppt or a similar threshold (Kroeger et al., 2017).

All four layers of data analytics indicated a moderate control of PAR on the CH_4 fluxes from the salt marshes (Tables 2–4, Figure 2). However, PAR was not statistically significant in the predictive modeling of CH_4 fluxes (see equation (7)). Therefore, the apparent influence of PAR on the CH_4 fluxes might have mostly reflected the temperature control on methanogenesis—which was demonstrated by the loadings of PAR, ST, and $NEE_{CH4,emission}$ on factor 1 (Table 3). Further, the weak biotic controls on the CH_4 fluxes of salt marshes could be attributed to high salinity, which might have substantially limited the effect of photosynthate and available labile carbon for methanogenesis. This finding is corroborated by our companion study that reported no notable linkages of CH_4 fluxes with plant variables such as aboveground biomass, belowground biomass, plant height, and stem density in the Sage Lot Pond (Moseman-Valtierra et al., 2016).

4.4. Control and Prediction of the Nighttime Net Respiration Fluxes of CO_2

The salt marshes in Cape Cod had notable nighttime net respiration fluxes (mean = 2.46 $\mu mol \cdot m^{-2} \cdot s^{-1}$, SD = 1.13 $\mu mol \cdot m^{-2} \cdot s^{-1}$; Table S3), which are in agreement with other salt marshes located in the Atlantic and Pacific Coasts of United States (Livesley & Andrusiak, 2012; Vivanco et al., 2015; Wigand et al., 2009). ST is considered the most important regulating factor of nighttime CO_2 respiration (autotrophic and heterotrophic) for various ecosystems (Davidson et al., 2012; Sierra, 2012; Tong et al., 2014; Xie et al., 2014). The temperature control on respiration is mainly characterized by accelerated microbial and enzyme activity in the substrate pool in response to increasing temperature (Pendall et al., 2004; Ryan & Law, 2005). We developed a power law-based model for the nighttime net respiration fluxes of CO_2 (i.e., $NEE_{CO2,emission}$) as a function of ST (equation (6)). The model suggested an important scaling relationship (expressed by using the "proportionality" sign) between respiration fluxes and ST with an approximate exponent of 3/2 (i.e., 1.5) as follows:

$$NEE_{CO2,emission} \propto ST^{3/2} \tag{8}$$

The emergent power law scaling model (equation (6)) can be considered an alternative for the classical Arrhenius-type exponential model (e.g., $NEE_{CO2,\,emission} = \alpha e^{\beta \cdot ST}$) of soil respiration (Lloyd & Taylor, 1994). To compare the two models, we estimated the exponential model with the growing season $NEE_{CO2,emission}$ and ST data (Table S3 in the supporting information) through a bootstrap Monte-Carlo procedure (10,000 iterations in both calibrations and validations; mean NSE = 0.80–0.85 and mean RSR = 0.39–0.43). The mean estimated values of α and β were 0.561 and 0.087, respectively; the parameters resulted in a mean temperature sensitivity (Q_{10}) value of 2.39 (calculated from $Q_{10} = e^{10\beta}$; see Lloyd & Taylor, 1994). The computed Q_{10} represented the reported range of 1.2–5.1 for *Spartina* sp. dominated wetlands across different seasons (Giurgevich & Dunn, 1979; Kirwan & Blum, 2011; Tong et al., 2014), as well as that for other tidal wetlands (dominated by *C. lasiocarpa* and *D. angustifolia*) and bogs (Hirota et al., 2006; Lafleur et al., 2005; Song et al., 2009). Further, conducting a synthesis of observed data from multiple ecosystems and species types, Lloyd and Taylor (1994) reported an overall Q_{10} value of 2.4, which is almost identical to our computed mean. Based on the mean statistics of our 10,000 estimations, the power law scaling model (NSE = 0.87–0.89 and RSR = 0.30–0.36) performed slightly better than the exponential model in predicting $NEE_{CO2,emission}$ for the nighttime temperature range of 10–25 °C in the four salt marshes of Cape Cod, MA.

4.5. Model Transferability and Scaling Across Salinity Regimes and Plant Communities

Although the emergent scaling-based power law models were developed using data that mostly represented polyhaline salt marshes (Table S3), the models may be used to scale the GHG fluxes from a range of coastal wetlands, representing different vegetation, tide, and salinity regimes (e.g., oligohaline, mesohaline, and

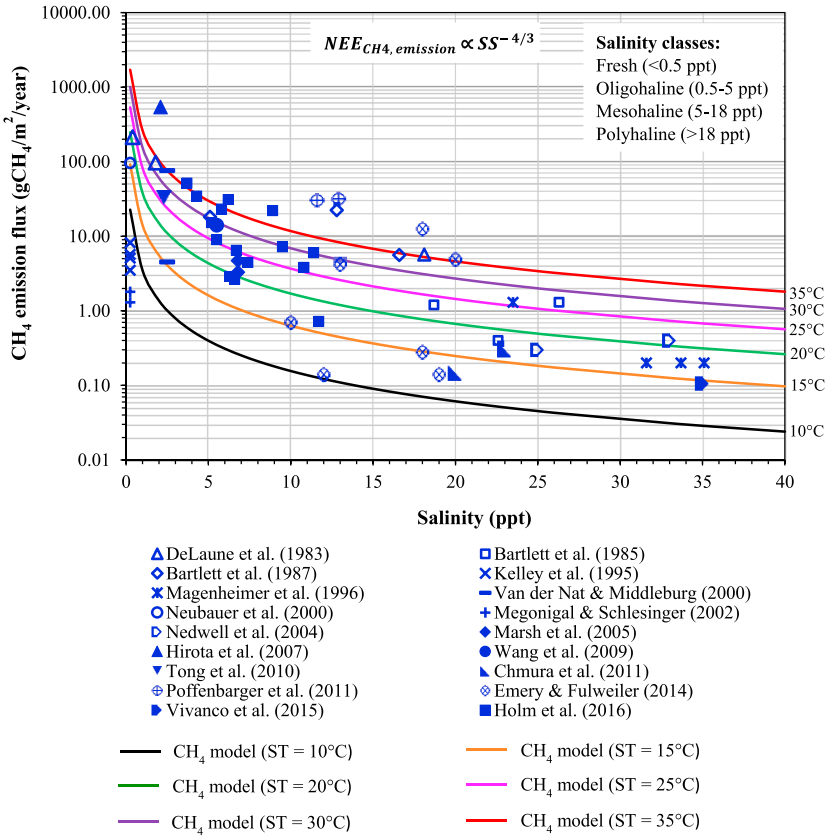

Figure 5. Comparison between modeled (using equation (7)) and literature-reported CH_4 emission fluxes across a wide range of salinity regimes and plant communities along the Atlantic, Gulf, and Pacific Coasts of United States and beyond (Canada, China, and Japan). $NEE_{CH4,emission}$ = net emission fluxes of CH_4; ST = soil temperature.

polyhaline). As an example, the scaling hypothesis was further investigated by comparing our model-predicted fluxes of CH_4 emission with observed data reported in literature (e.g., Bartlett et al., 1985, 1987; Chmura et al., 2011; DeLaune et al., 1983; Emery & Fulweiler, 2014; Hirota et al., 2007; Holm et al., 2016; Kelley et al., 1995; Magenheimer et al., 1996; Marsh et al., 2005; Megonigal & Schlesinger, 2002; Nedwell et al., 2004; Neubauer et al., 2000; Poffenbarger et al., 2011; Tong et al., 2010; Van der Nat & Middleburg, 2000; Vivanco et al., 2015; Wang et al., 2009), incorporating a salinity range of 0.25–40 ppt. The data sets represented a wide range of dominant wetland plant communities (e.g., *Acer rubrum*, *P. australis*, *Panisum hemitomon*, and *S. alterniflora*), soil surface flooding (flooded versus non-flooded), and measurement methods (light versus dark, as well as light + dark chambers) across the Atlantic, Gulf, and Pacific Coasts of United States and beyond (Canada, China, and Japan). In this test, CH_4 fluxes were predicted using equation (7) by varying the salinity from 0.25 to 40 ppt for six reference STs (10, 15, 20, 25, 30, and 35 °C). Further, the predicted fluxes ($nmol \cdot m^{-2} \cdot s^{-1}$) were converted to annual fluxes ($gCH_4 \cdot m^{-2} \cdot year^{-1}$; 1 $nmol \cdot m^{-2} \cdot s^{-1}$ = 0.5046 $gCH_4 \cdot m^{-2} \cdot year^{-1}$) to be consistent with the units of Poffenbarger et al. (2011). The model reasonably represented the observed CH_4 fluxes for polyhaline (>18 ppt), mesohaline (5–18 ppt), oligohaline (0.5–5 ppt), and freshwater (0.25–0.5 ppt) wetlands, incorporating a geographic gradient in vegetation and tidal hydrology (Figure 5). The analysis further suggested an emergent scaling relationship of wetland CH_4 emissions with the porewater salinity with an exponent of approximately 4/3 (i.e., ~1.35) for a range of ST as follows:

$$NEE_{CH\,4,emission} \propto SS^{-4/3} \tag{9}$$

The emergent scaling relationships (equations (7) and (9)) indicated an intertwined effect of salinity and temperature on production and emission of CH_4 fluxes in coastal salt marshes. The CH_4 fluxes increased

Table 5
The Projected Increases in Environmental Drivers and the Greenhouse Gas Fluxes by 2050 and 2080 Based on the Ensemble Averages of 20 Downscaled General Circulation Models for the Waquoit Bay and Adjacent Estuaries Under the Intergovernmental Panel on Climate Change Scenarios of RCP 4.5 and 8.5

		Projected increase			
Model variables	Baseline year 2013	RCP 4.5 2050	RCP 8.5 2050	RCP 4.5 2080	RCP 8.5 2080
PAR	1,468.8 $\mu mol{\cdot}m^{-2}{\cdot}s^{-1}$	2.2%	2.2%	2.7%	2.5%
ST	20 °C	1.2 °C	1.6 °C	1.9 °C	3.1 °C
SS	29 ppt	10.0%	10.0%	21.0%	21.0%
$NEE_{CO2,uptake}$	-6.35 $\mu mol{\cdot}m^{-2}{\cdot}s^{-1}$	10.5%	18.9%	14.4%	33.9%
$NEE_{CO2,emission}$	3.23 $\mu mol{\cdot}m^{-2}{\cdot}s^{-1}$	8.7%	12.4%	14.6%	23.8%
$NEE_{CH4,emission}$	0.83 $nmol{\cdot}m^{-2}{\cdot}s^{-1}$	8.0%	16.4%	10.0%	30.0%
NACR (GWP = 34)	-290.63 $gC.m^{-2}$	12.6%	25.8%	14.4%	44.9%
NACR (GWP = 86)	-282.44 $gC.m^{-2}$	9.6%	22.5%	11.4%	41.2%

Note. $NEE_{CO2,uptake}$, $NEE_{CO2,emission}$, $NEE_{CH4,emission}$, NACR, PAR, ST, and SS refer to the daytime net uptake fluxes of CO_2, net emission fluxes of CO_2, net emission fluxes of CH_4, net atmospheric carbon removal, photosynthetically active radiation, soil temperature, and porewater salinity, respectively; ppt refers to parts per thousand. GWP refers to CO_2 equivalent global warming potential for CH_4. The baseline and projected $NEE_{CO2,uptake}$, $NEE_{CO2,emission}$, and $NEE_{CH4,emission}$ were computed by using equations (5)–(7), respectively. Negative indicates the net uptake fluxes of CO_2. NACR is the difference between net carbon (CO_2) uptake and net carbon (CO_2 and CH_4) emissions in the salt marshes. NACR was calculated by upscaling the greenhouse gas fluxes over the growing season (May–October; 183 days) in units of gram carbon (C) per square meter marsh area. RCP = Representative Concentration Pathway.

nonlinearly with lower salinity toward the oligohaline and freshwater marshes, and the emissions at the same salinity were notably higher at higher temperatures (Figure 5). The similarity between predictions and observations of CH_4 emission, as well as that between predictions from the power law and classical Arrhenius models of net CO_2 respiration, provided important evidence of potential model extrapolations and scaling across a large range of salinity regimes and plant communities.

4.6. Implications of Climate Change, Sea Level Rise, and Caveats

We explored the potential scenarios of GHG fluxes for our study area under a changing climate and rising sea level. For example, the Intergovernmental Panel on Climate Change (IPCC) RCP4.5 and 8.5 represent moderate and very high emission scenarios, respectively (IPCC, 2014). Based on observations (Table 1), the baseline 2013 values for PAR, ST, and SS were considered to be 1,468.8 $\mu mol \cdot m^{-2} \cdot s^{-1}$, 20 °C, and 29 ppt, respectively. Ensemble averages of the downscaled scenarios from 20 general circulation models (GCMs; Table S6 in the supporting information; Abatzoglou & Brown, 2012; United States Geological Survey [USGS], 2017) for Waquoit Bay and adjacent estuaries suggested an increase of PAR by approximately 2% in 2050 and 3% in 2080, relative to the 2013 values (Table 5). The projected increase in temperature was approximately 1–1.5 °C by 2050 and 2–3 °C by 2080. Based on the IPCC scenarios for sea level rise (SLR), salinity was anticipated to increase from the 2013 baseline by 10% in 2050 and 21% in 2080. This assumption of increasing salinity with SLR in estuarine ecosystems is supported by previous studies (Cloern et al., 2011; Hilton et al., 2008; Morris, 1995; Schile et al., 2017). Although sediment accretion and increased belowground biomass may significantly compensate the rising level (Cherry et al., 2009; Morris et al., 2002; Schile et al., 2014), tidal wetlands are expected to experience a net loss in relative elevation (Schile et al., 2017). Overall, SLR could increase the extent, frequency, and duration of tidal flooding, leading to a higher salinity in the coastal salt marshes.

Assuming persistence of the salt marshes and plant species under a warming climate and SLR in the future, we calculated the anticipated changes in GHG fluxes for the salt marshes by using the 2013 baseline and the downscaled scenarios of PAR, ST, and SS for 2050 and 2080 as inputs to the predictive models (equations (5)–(7)). The inputs led to the baseline (2013) fluxes of -6.35 $\mu mol \cdot m^{-2} \cdot s^{-1}$ for daytime CO_2 uptake, 3.23 $\mu mol \cdot m^{-2} \cdot s^{-1}$ for nighttime CO_2 respiration, and 0.83 $nmol \cdot m^{-2} \cdot s^{-1}$ for CH_4 emission (Table 5). The 2013 baseline NACR over the growing season (May–October) was estimated to be -290.63 and -282.44 gC/m^2 by using, respectively, 34 and 86 as the global warming potential of CH_4 (Myhre et al., 2013). Based on the downscaled scenarios of 20 GCMs (RCP 4.5 and 8.5) and projected SLR, the ensemble

average of the daytime net uptake fluxes of CO_2 would increase from their 2013 baseline estimations by approximately 11–19% in 2050 and 14–34% in 2080 (Table 5). In contrast, the nighttime net respiration fluxes of CO_2 would increase by approximately 9–12% in 2050 and 15–24% in 2080. Further, the ensemble average of CH_4 emissions would increase by approximately 8–16% in 2050 and 10–30% in 2080. The multimodel ensemble average of NACR was projected to increase by approximately 10–26% in 2050 and 11–45% in 2080 among the two RCP scenarios and global warming potentials. Overall, the differences in the baseline fluxes of net CO_2 uptake and respiration, as well as their projected increases, indicated the potential for salt marshes in Waquoit Bay and adjacent areas to accelerate the removal of atmospheric CO_2 under a warming climate and rising sea level. However, the assumption of persistent salt marshes and plant species under the future climate and sea level should be considered as a caveat for this analysis. The projected estimations can further be impacted if temperature and salinity exceed plants' tolerable thresholds of physiological and environmental stresses under extreme climate. We recommend further investigations with larger observational data sets to determine whether the salt marshes would indeed continue to stock carbon at the current or at a higher rate in the future.

The successful predictions of the GHG fluxes across the four sites (Figure 4) with a single set of parameters suggested spatial robustness of the emergent power law scaling models (equations (5)–(7)) in Waquoit Bay and adjacent region. However, the models should be tested with new data from additional salt marshes along a larger gradient of nitrogen, salinity, and tidal flooding to expand application to the regional scale (e.g., New England) and beyond. Specifically, model applications at wetlands with much higher N loading rates than our study sites should be considered with caveats. The current models were developed by using the measured data for the extended growing season (May–October) of 2013. The interannual variability of GHG fluxes and the environmental predictors had not been incorporated into the current models. The net lateral fluxes of carbon between the tidal marshes and the bay were not modeled in this study due to the lack of relevant observational data. However, measurements and modeling of net lateral fluxes are challenging and highly uncertain (Wang et al., 2016), meriting a separate investigation. Subject to the availability of data, future research can further indicate whether porewater salinity should be considered as a predictor (in addition to ST) for the nighttime CO_2 respiration model. The next-generation models could also account for variation in plant factors (i.e., biomass and leaf area) to predict the GHG fluxes at longer time scales (e.g., monthly and annual).

In general, mathematical modeling is an abstraction of reality, and many complex processes are simplified in the abstraction methods. Depending on the data quality and quantity, a conventional statistical analysis and empirical modeling may lead to results that lack ecological underpinning and contradict mechanistic understanding. In our study, the filtering methods ensured a good quality and adequacy of the data sets by excluding only 12–25% of the corresponding primary data (section 2.2). We also employed a four-layer data analytics approach (correlation matrix, PCA, FA, and PLSR) and synthesized their overall outcomes so that the limitations and artifacts from any particular methods would not misguide the overall pursuit of determining the environmental controls of salt marsh GHG fluxes. Further, the identified major controls of the GHG fluxes, as well as their nonlinear scaling relationships with PAR, ST, and SS were mechanistically explained based on existing literature (sections 4.2–4.5). The "emergent scaling" hypothesis of this study has, therefore, a potentially far-reaching ecological and biogeochemical significance, specifically pertaining to the development of generalized (scale-invariant) predictive models of GHG fluxes in a wide range of coastal wetlands.

Given the lack of observations and predictive tools, the presented emergent power law-based scaling models can be considered a step forward toward developing relatively simple, mechanistically meaningful, and parsimonious models to predict the major GHG fluxes and NACR in coastal salt marshes. Further, in the absence or scarcity of observed GHG fluxes (which is often the case for tidal marshes), the empirical models can be used to estimate data that can guide the calibration and validation of complex process models (Abramowitz et al., 2007; Beer et al., 2010; Keenan et al., 2012). The empirical models, therefore, can also be used as diagnostic tools and data benchmarks to develop low-dimensional, reliable process models (Stoy et al., 2005) to mechanistically predict GHG fluxes and carbon storage in coastal salt marshes.

5. Conclusions

We determined the relative environmental controls and emergent scaling of CO_2 and CH_4 fluxes in coastal salt marshes by conducting data analytics and empirical modeling. Our measurements from four salt

marshes in Waquoit Bay and adjacent estuaries at Cape Cod, MA exhibited high net CO_2 uptake and low CH_4 emissions during May–October 2013. However, the GHG fluxes did not significantly vary with the nitrogen loading gradient (5–126 $kg \cdot ha^{-1} \cdot year^{-1}$) across the salt marshes (p value = 0.41–0.71). Soil temperature (ST) was the strongest driver of both fluxes, having approximately 2 and 4–5 times stronger influence than that of PAR and porewater salinity, respectively. Porewater pH was at or near neutral, exhibiting no notable control on the GHG fluxes. Further, hydrologic variables such as well water level and soil moisture did not have a direct predictive control on the GHG fluxes, although both fluxes were significantly higher during the high tides than the low tides (p value < 0.001). However, soil moisture was high and mostly remained at or near saturation due to semidiurnal tidal flooding, which might have indirectly influenced the GHG fluxes by contributing to the temporal variation of salinity and ST. On average, the aggregated "climatic" process component (PAR and ST) exhibited approximately 5 and 13 times stronger controls on the GHG fluxes than that of the "biogeochemical" (pH and salinity) and "hydrologic" (water level and soil moisture) components in these salt marshes at Cape Cod.

The findings on dominant controls were leveraged to investigate the emergent scaling of salt marsh CO_2 and CH_4 fluxes and develop power law-based scaling models to accurately predict the GHG fluxes based on a small set of statistically significant environmental drivers (NSE = 0.80–0.91; RSR = 0.30–0.49). The daytime net CO_2 uptake fluxes were predicted from PAR, ST, and porewater salinity, whereas only ST and salinity appeared significant to predict the day or nighttime CH_4 emission fluxes. However, the nighttime net respiration fluxes of CO_2 were predicted as a power law scaling function of ST, which performed slightly better than the classical Arrhenius-type exponential model of soil respiration (Lloyd & Taylor, 1994). Further, comparison of the predicted CH_4 fluxes with observations from literature (e.g., Chmura et al., 2011; Emery & Fulweiler, 2014; Holm et al., 2016; Poffenbarger et al., 2011; Vivanco et al., 2015) provided promising evidences of potential scaling and model extrapolations across a wide range of salinity regimes and plant communities along the Atlantic, Gulf, and Pacific Coasts of United States and beyond (Canada, China, and Japan). Subject to the availability of new observations for fluxes and the environmental drivers, model scaling and generalization should further be tested across large biological, ecological, biogeochemical, hydroclimatic, and geographical gradients in future research.

The emergent scaling based predictive models were represented in a user-friendly Excel spreadsheet for a broader community of scientists and end users. The models and Excel software serve as ecological engineering tools to explore scenarios of salt marsh GHG fluxes and NACR in Waquoit Bay and adjacent region under a changing climate (PAR and temperature) and rising sea level (increased tidal flooding and porewater salinity). For example, using the downscaled climatic projections (PAR and temperature) from 20 GCMs and anticipated sea level (salinity) as inputs into the models, the salt marshes of Cape Cod were projected to remove a higher (than current) rate of atmospheric carbon in 2050 and 2080. Analysis of such scenarios may help the coastal stakeholders (e.g., reserve managers, restoration practitioners, and policymakers) to formulate guidelines for restoration, monitoring, and maintenance of the tidal salt marshes under a changing climate and environment.

Acknowledgments
This research was funded by the NOAA National Estuarine Research Reserve Science Collaborative (NA09NOS4190153 and NA14NOS4190145), awarded to Abdul-Aziz, Tang, Moseman-Valtierra, and Kroeger. Abdul-Aziz and Ishtiaq were substantially supported by grants from NSF, awarded to Abdul-Aziz (NSF CBET Environmental Sustainability Award No. 1705941 and 1561941/1336911). Participation of USGS scientists was supported by the USGS LandCarbon Program. We are grateful to Tonna-Marie Surgeon-Rogers, James Rassman, and Alison Leschen of Waquoit Bay National Estuarine Research Reserve for participating in interesting discussion during the conception and execution of this research. Our thanks go to Jessie Gunnard, Karissa Parker, Lauren Krohmer, and Mike Callahan for their hard work in the field. We kindly thank the four anonymous reviewers, Associate Editor, and Editor for providing constructive and insightful comments on the primary manuscript. Data used in this study are described in main text, figures, tables, and the supporting information. Further, the complete data set is available at https://sites.google.com/view/ecological-water/data-and-models. Any use of trade, firm, or product names is for descriptive purposes only, and does not imply endorsement by the United States Government.

References

Abatzoglou, J. T., & Brown, T. J. (2012). A comparison of statistical downscaling methods suited for wildfire applications. *International Journal of Climatology*, *32*(5), 772–780. https://doi.org/10.1002/joc.2312

Abramowitz, G., Pitman, A., Gupta, H., Kowalczyk, E., & Wang, Y. (2007). Systematic bias in land surface models. *Journal of Hydrometeorology*, *8*(5), 989–1001. https://doi.org/10.1175/JHM628.1

Akaike, H. (1974). A new look at the statistical model identification. *IEEE Transactions on Automatic Control*, *19*(6), 716–723. https://doi.org/10.1109/TAC.1974.1100705

Bartlett, K. B., Bartlett, D. S., Harriss, R. C., & Sebacher, D. I. (1987). Methane emissions along a salt marsh salinity gradient. *Biogeochemistry*, *4*(3), 183–202. https://doi.org/10.1007/BF02187365

Bartlett, K. B., Harriss, R. C., & Sebacher, D. I. (1985). Methane flux from coastal salt marshes. *Journal of Geophysical Research*, *90*, 5710–5720. https://doi.org/10.1029/JD090iD03p05710

Beer, C., Reichstein, M., Tomelleri, E., Ciais, P., Jung, M., Carvalhais, N., et al. (2010). Terrestrial gross carbon dioxide uptake: Global distribution and covariation with climate. *Science*, *329*(5993), 834–838. https://doi.org/10.1126/science.1184984

Blöschl, G., & Sivapalan, M. (1995). Scale issues in hydrological modelling: A review. *Hydrological Processes*, *9*(3–4), 251–290. https://doi.org/10.1002/hyp.3360090305

Born, M., DÖrr, H., & Levin, I. (1990). Methane consumption in aerated soils of the temperate zone. *Tellus B*, *42*(1), 2–8. https://doi.org/10.3402/tellusb.v42i1.15186

Bradley, P. M., & Morris, J. T. (1990). Influence of oxygen and sulfide concentration on nitrogen uptake kinetics in Spartina alterniflora. *Ecology*, *71*(1), 282–287. https://doi.org/10.2307/1940267

Bridgham, S. D., Patrick Megonigal, J., Keller, J. K., Bliss, N. B., & Trettin, C. (2006). The carbon balance of North American wetlands. *Wetlands*, *26*(4), 889–916. https://doi.org/10.1672/0277-5212(2006)26[889:TCBONA]2.0.CO;2

Brown, C. E., Pezeshki, S. R., & DeLaune, R. D. (2006). The effects of salinity and soil drying on nutrient uptake and growth of *Spartina alterniflora* in a simulated tidal system. *Environmental and Experimental Botany*, *58*(1-3), 140–148. https://doi.org/10.1016/j.envexpbot.2005.07.006

Burke, D. J., Hamerlynck, E. P., & Hahn, D. (2002). Interactions among plant species and microorganisms in salt marsh sediments. *Applied and Environmental Microbiology*, *68*(3), 1157–1164. https://doi.org/10.1128/AEM.68.3.1157-1164.2002

Callaway, J. C., Thomas Parker, V., Vasey, M. C., & Schile, L. M. (2007). Emerging issues for the restoration of tidal marsh ecosystems in the context of predicted climate change. *Madrono*, *54*(3), 234–248. https://doi.org/10.3120/0024-9637(2007)54[234:EIFTRO]2.0.CO;2

Cao, M., Marshall, S., & Gregson, K. (1996). Global carbon exchange and methane emissions from natural wetlands: Application of a process-based model. *Journal of Geophysical Research*, *101*, 14,399–14,414. https://doi.org/10.1029/96JD00219

Charles, H., & Dukes, J. S. (2009). Effects of warming and altered precipitation on plant and nutrient dynamics of a New England salt marsh. *Ecological Applications*, *19*(7), 1758–1773. https://doi.org/10.1890/08-0172.1

Cherry, J. A., McKee, K. L., & Grace, J. B. (2009). Elevated CO2 enhances biological contributions to elevation change in coastal wetlands by offsetting stressors associated with sea-level rise. *Journal of Ecology*, *97*(1), 67–77. https://doi.org/10.1111/j.1365-2745.2008.01449.x

Chmura, G. L., Kellman, L., & Guntenspergen, G. R. (2011). The greenhouse gas flux and potential global warming feedbacks of a northern macrotidal and microtidal salt marsh. *Environmental Research Letters*, *6*(4), 044016. https://doi.org/10.1088/1748-9326/6/4/044016

Cloern, J. E., Knowles, N., Brown, L. R., Cayan, D., Dettinger, M. D., Morgan, T. L., et al. (2011). Projected evolution of California's San Francisco Bay-Delta-river system in a century of climate change. *PLoS One*, *6*(9), e24465. https://doi.org/10.1371/journal.pone.0024465

Coastal Wetland GHG Model (CWGM) (2018). Coastal wetlands greenhouse gas prediction model software. Available online at https://sites.google.com/view/ecological-water/data-and-models

Cole, M. L., Kroeger, K. D., McClelland, J. W., & Valiela, I. (2005). Macrophytes as indicators of land-derived wastewater: Application of $\delta 1^5$N method in aquatic systems. *Water Resources Research*, *41*, W01014. https://doi.org/10.1029/2004WRR003269

Conrad, R. (1989). Control of methane production in terrestrial ecosystems. In M. O. Andreae, & D. S. Schimel (Eds.), *Exchange of trace gases between terrestrial ecosystems and the atmosphere*, *Dahlem Workshop Reports*, (pp. 39–58). UK: Wiley Chichester.

Couto, T., Duarte, B., Martins, I., Caçador, I., & Marques, J. C. (2014). Modelling the effects of global temperature increase on the growth of salt marsh plants. *Applied Ecology and Environmental Research*, *12*(3), 753–764. https://doi.org/10.15666/aeer/1203_753764

Crooks, S., Emmett-Mattox, S., & Findsen, J. (2010). Findings of the National Blue Ribbon Panel on the Development of a Greenhouse Gas Offset Protocol for Tidal Wetlands Restoration and Management: Action plan to guide protocol development. *Restore America's Estuaries, Philip Williams & Associates, Ltd.,* and Science Applications International Corporation.

Davidson, E. A., Samanta, S., Caramori, S. S., & Savage, K. (2012). The Dual Arrhenius and Michaelis–Menten kinetics model for decomposition of soil organic matter at hourly to seasonal time scales. *Global Change Biology*, *18*(1), 371–384. https://doi.org/10.1111/j.1365-2486.2011.02546.x

Davies, J. L. (1964). A morphogenic approach to world shorelines. *Zeitschrift für Geomorphologie*, *8*, 127–142.

De Jong, S. (1993). SIMPLS: An alternative approach to partial least squares regression. *Chemometrics and Intelligent Laboratory Systems*, *18*(3), 251–263. https://doi.org/10.1016/0169-7439(93)85002-X

DeLaune, R. D., Smith, C. J., & Patrick, W. H. (1983). Methane release from Gulf coast wetlands. *Tellus B*, *35*(1), 8–15.

Dunfield, P., Dumont, R., & Moore, T. R. (1993). Methane production and consumption in temperate and subarctic peat soils: Response to temperature and pH. *Soil Biology and Biochemistry*, *25*(3), 321–326. https://doi.org/10.1016/0038-0717(93)90130-4

Emery, H. E., & Fulweiler, R. W. (2014). *Spartina alterniflora* and invasive *Phragmites australis* stands have similar greenhouse gas emissions in a New England marsh. *Aquatic Botany*, *116*, 83–92. https://doi.org/10.1016/j.aquabot.2014.01.010

Enquist, B. J., Economo, E. P., Huxman, T. E., Allen, A. P., Ignace, D. D., & Gillooly, J. F. (2003). Scaling metabolism from organisms to ecosystems. *Nature*, *423*(6940), 639–642. https://doi.org/10.1038/nature01671

Ewing, K., McKee, K., Mendelssohn, I., & Hester, M. (1995). A comparison of indicators of sublethal salinity stress in the salt marsh grass, *Spartina patens* (Ait.) Muhl. *Aquatic Botany*, *52*(1–2), 59–74. https://doi.org/10.1016/0304-3770(95)00487-K

Fan, Z., David McGuire, A., Turetsky, M. R., Harden, J. W., Michael Waddington, J., & Kane, E. S. (2013). The response of soil organic carbon of a rich fen peatland in interior Alaska to projected climate change. *Global Change Biology*, *19*(2), 604–620. https://doi.org/10.1111/gcb.12041

Farrior, C. E., Bohlman, S. A., Hubbell, S., & Pacala, S. W. (2016). Dominance of the suppressed: Power-law size structure in tropical forests. *Science*, *351*(6269), 155–157. https://doi.org/10.1126/science.aad0592

Frolking, S., & Crill, P. (1994). Climate controls on temporal variability of methane flux from a poor fen in southeastern New Hampshire: Measurement and modeling. *Global Biogeochemical Cycles*, *8*, 385–397. https://doi.org/10.1029/94GB01839

Giurgevich, J. R., & Dunn, E. L. (1979). Seasonal patterns of CO_2 and water vapor exchange of the tall and short height forms of *Spartina alterniflora* Loisel in a Georgia salt marsh. *Oecologia*, *43*(2), 139–156. https://doi.org/10.1007/BF00344767

Guan, Q., Chen, J., Wei, Z., Wang, Y., Shiyomi, M., & Yang, Y. (2016). Analyzing the spatial heterogeneity of number of plant individuals in grassland community by using power law model. *Ecological Modelling*, *320*, 316–321. https://doi.org/10.1016/j.ecolmodel.2015.10.019

Guo, H., Noormets, A., Zhao, B., Chen, J., Sun, G., Gu, Y., et al. (2009). Tidal effects on net ecosystem exchange of carbon in an estuarine wetland. *Agricultural and Forest Meteorology*, *149*(11), 1820–1828. https://doi.org/10.1016/j.agrformet.2009.06.010

Hilton, T. W., Najjar, R. G., Zhong, L., & Li, M. (2008). Is there a signal of sea-level rise in Chesapeake Bay salinity? *Journal of Geophysical Research*, *113*, C09002. https://doi.org/10.1029/2007JC004247

Hirota, M., Senga, Y., Seike, Y., Nohara, S., & Kunii, H. (2007). Fluxes of carbon dioxide, methane and nitrous oxide in two contrastive fringing zones of coastal lagoon, Lake Nakaumi, Japan. *Chemosphere*, *68*(3), 597–603. https://doi.org/10.1016/j.chemosphere.2007.01.002

Hirota, M., Tang, Y., Hu, Q., Hirata, S., Kato, T., Mo, W., et al. (2006). Carbon dioxide dynamics and controls in a deep-water wetland on the Qinghai-Tibetan Plateau. *Ecosystems*, *9*(4), 673–688. https://doi.org/10.1007/s10021-006-0029-x

Holm, G. O., Perez, B. C., McWhorter, D. E., Krauss, K. W., Johnson, D. J., Raynie, R. C., & Killebrew, C. J. (2016). Ecosystem level methane fluxes from tidal freshwater and brackish marshes of the Mississippi River Delta: Implications for coastal wetland carbon projects. *Wetlands*, *36*(3), 401–413. https://doi.org/10.1007/s13157-016-0746-7

Hondzo, M., Voller, V. R., Morris, M., Foufoula-Georgiou, E., Finlay, J., Ganti, V., & Power, M. E. (2013). Estimating and scaling stream ecosystem metabolism along channels with heterogeneous substrate. *Ecohydrology*, *6*(4), 679–688. https://doi.org/10.1002/eco.1391

Howarth, R. W. (1993). Microbial processes in salt-marsh sediments. In T. E. Ford (Ed.), *Aquatic microbiology: An ecological approach*, (pp. 239–259). Malden, Mass: Blackwell.

Howes, B. L., Dacey, J. W. H., & Goehringer, D. D. (1986). Factors controlling the growth form of Spartina alterniflora: Feedbacks between above-ground production, sediment oxidation, nitrogen and salinity. *The Journal of Ecology*, *74*(3), 881–898. https://doi.org/10.2307/2260404

Idaszkin, Y. L., & Bortolus, A. (2011). Does low temperature prevent *Spartina alterniflora* from expanding toward the austral-most salt marshes? *Plant Ecology*, *212*(4), 553–561. https://doi.org/10.1007/s11258-010-9844-4

Inglett, K. S., Inglett, P. W., Reddy, K. R., & Osborne, T. Z. (2012). Temperature sensitivity of greenhouse gas production in wetland soils of different vegetation. *Biogeochemistry*, *108*(1–3), 77–90. https://doi.org/10.1007/s10533-011-9573-3

Intergovernmental Panel on Climate Change (2014). *Climate change 2014: Synthesis report. Contribution of Working Groups I, II and III to the Fifth Assessment Report of the Intergovernmental Panel on Climate Change* (Core Writing Team, R.K. Pachauri and L.A. Meyer [eds.]). IPCC, Geneva, Switzerland, 151.

Ishtiaq, K. S., & Abdul-Aziz, O. I. (2015). Relative linkages of canopy-level CO_2 fluxes with the climatic and environmental variables for US deciduous forests. *Environmental Management*, *55*(4), 943–960. https://doi.org/10.1007/s00267-014-0437-1

Ishtiaq, K. S., & Abdul-Aziz, O. I. (2017). A generalized model of hourly net ecosystem exchange (NEE) for Florida Everglades freshwater wetlands. *Wetlands*, *37*(5), 925–939. https://doi.org/10.1007/s13157-017-0928-y

Jansson, P. E. (2012). CoupModel: Model use, calibration, and validation. *Transactions of the ASABE*, *55*(4), 1337–1346. https://doi.org/10.13031/2013.42245

Jolliffe, I. T. (1993). Principal component analysis: A beginner's guide—II. Pitfalls, myths and extensions. *Weather*, *48*(8), 246–253. https://doi.org/10.1002/j.1477-8696.1993.tb05899.x

Juszczak, R., Acosta, M., & Olejnik, J. (2012). Comparison of daytime and nighttime ecosystem respiration measured by the closed chamber technique on a temperate mire in Poland. *Polish Journal of Environmental Studies*, *21*(3), 643–568.

Keenan, T. F., Davidson, E., Moffat, A. M., Munger, W., & Richardson, A. D. (2012). Using model-data fusion to interpret past trends, and quantify uncertainties in future projections, of terrestrial ecosystem carbon cycling. *Global Change Biology*, *18*(8), 2555–2569. https://doi.org/10.1111/j.1365-2486.2012.02684.x

Kelley, C. A., Martens, C. S., & Ussler, W. (1995). Methane dynamics across a tidally flooded riverbank margin. *Limnology and Oceanography*, *40*(6), 1112–1129. https://doi.org/10.4319/lo.1995.40.6.1112

Kirwan, M. L., & Blum, L. K. (2011). Enhanced decomposition offsets enhanced productivity and soil carbon accumulation in coastal wetlands responding to climate change. *Biogeosciences*, *8*(4), 987–993. https://doi.org/10.5194/bg-8-987-2011

Kroeger, K. D., Cole, M. L., & Valiela, I. (2006). Groundwater-transported dissolved organic nitrogen exports from coastal watersheds. *Limnology and Oceanography*, *51*(5), 2248–2261. https://doi.org/10.4319/lo.2006.51.5.2248

Kroeger, K. D., Crooks, S., Moseman-Valtierra, S., & Tang, J. (2017). Restoring tides to reduce methane emissions in impounded wetlands: A new and potent blue carbon climate change intervention. *Scientific Reports*, *7*(1), 11914. https://doi.org/10.1038/s41598-017-12138-4

Kubien, D. S., von Caemmerer, S., Furbank, R. T., & Sage, R. F. (2003). C_4 photosynthesis at low temperature. A study using transgenic plants with reduced amounts of Rubisco. *Plant Physiology*, *132*(3), 1577–1585. https://doi.org/10.1104/pp.103.021246

Kuhn, M., & Johnson, K. (2013). *Applied predictive modeling*. New York: Springer. https://doi.org/10.1007/978-1-4614-6849-3

Lafleur, P. M., Moore, T. R., Roulet, N. T., & Frolking, S. (2005). Ecosystem respiration in a cool temperate bog depends on peat temperature but not water table. *Ecosystems*, *8*(6), 619–629. https://doi.org/10.1007/s10021-003-0131-2

Lamers, L. P., Govers, L. L., Janssen, I. C., Geurts, J. J., Van der Welle, M. E., Van Katwijk, M. M., et al. (2013). Sulfide as a soil phytotoxin—A review. *Frontiers in Plant Science*, *4*. https://doi.org/10.3389/fpls.2013.00268

Lewis, M. A., & Weber, D. E. (2002). Effects of substrate salinity on early seedling survival and growth of *Scirpus robustus* Pursh and *Spartina alterniflora* Loisel. *Ecotoxicology*, *11*(1), 19–26. https://doi.org/10.1023/A:1013788928922

Livesley, S. J., & Andrusiak, S. M. (2012). Temperate mangrove and salt marsh sediments are a small methane and nitrous oxide source but important carbon store. *Estuarine, Coastal and Shelf Science*, *97*, 19–27. https://doi.org/10.1016/j.ecss.2011.11.002

Lloyd, J., & Taylor, J. A. (1994). On the temperature dependence of soil respiration. *Functional Ecology*, *8*(3), 315–323. https://doi.org/10.2307/2389824

Macreadie, P. I., Nielsen, D. A., Kelleway, J. J., Atwood, T. B., Seymour, J. R., Petrou, K., et al. (2017). Can we manage coastal ecosystems to sequester more blue carbon? *Frontiers in Ecology and the Environment*, *15*(4), 206–213. https://doi.org/10.1002/fee.1484

Magenheimer, J. F., Moore, T. R., Chmura, G. L., & Daoust, R. J. (1996). Methane and carbon dioxide flux from a macrotidal salt marsh, Bay of Fundy, New Brunswick. *Estuaries*, *19*(1), 139–145. https://doi.org/10.2307/1352658

Mahecha, M. D., Reichstein, M., Carvalhais, N., Lasslop, G., Lange, H., Seneviratne, S. I., et al. (2010). Global convergence in the temperature sensitivity of respiration at ecosystem level. *Science*, *329*(5993), 838–840. https://doi.org/10.1126/science.1189587

Mantlana, K. B., Arneth, A., Veenendaal, E. M., Wohland, P., Wolski, P., Kolle, O., et al. (2008). Photosynthetic properties of C_4 plants growing in an African savanna/wetland mosaic. *Journal of Experimental Botany*, *59*(14), 3941–3952. https://doi.org/10.1093/jxb/ern237

Maricle, B. R., & Lee, R. W. (2007). Root respiration and oxygen flux in salt marsh grasses from different elevational zones. *Marine Biology*, *151*(2), 413–423. https://doi.org/10.1007/s00227-006-0493-z

Marsh, A. S., Rasse, D. P., Drake, B. G., & Megonigal, J. P. (2005). Effect of elevated CO2 on carbon pools and fluxes in a brackish marsh. *Estuaries*, *28*(5), 694–704. https://doi.org/10.1007/BF02732908

Martin, R. M., & Moseman-Valtierra, S. (2017). Different short-term responses of greenhouse gas fluxes from salt marsh mesocosms to simulated global change drivers. *Hydrobiologia*, *802*(1), 71–83. https://doi.org/10.1007/s10750-017-3240-1

Mateos-Naranjo, E., Redondo-Gómez, S., Álvarez, R., Cambrollé, J., Gandullo, J., & Figueroa, M. E. (2010). Synergic effect of salinity and CO_2 enrichment on growth and photosynthetic responses of the invasive cordgrass *Spartina densiflora*. *Journal of Experimental Botany*, *61*(6), 1643–1654. https://doi.org/10.1093/jxb/erq029

Mcleod, E., Chmura, G. L., Bouillon, S., Salm, R., Björk, M., Duarte, C. M., et al. (2011). A blueprint for blue carbon: Toward an improved understanding of the role of vegetated coastal habitats in sequestering CO_2. *Frontiers in Ecology and the Environment*, *9*(10), 552–560. https://doi.org/10.1890/110004

Megonigal, J. P., & Schlesinger, W. (2002). Methane-limited methanotrophy in tidal freshwater swamps. *Global Biogeochemical Cycles*, *16*(4), 1088. https://doi.org/10.1029/2001GB001594

Melton, J. R., Wania, R., Hodson, E. L., Poulter, B., Ringeval, B., Spahni, R., et al. (2013). Present state of global wetland extent and wetland methane modelling: Conclusions from a model intercomparison project (WETCHIMP). *Biogeosciences*, *10*(2), 753–788. https://doi.org/10.5194/bg-10-753-2013

Mendelssohn, I. A., & McKee, K. L. (1988). Spartina alterniflora die-back in Louisiana: Time-course investigation of soil waterlogging effects. *The Journal of Ecology*, *76*(2), 509–521. https://doi.org/10.2307/2260609

Morris, J. T. (1995). The mass balance of salt and water in intertidal sediments: Results from North Inlet, South Carolina. *Estuaries and Coasts*, *18*(4), 556–567. https://doi.org/10.2307/1352376

Morris, J. T. (2000). Effects of sea level anomalies on estuarine processes. In *Estuarine science: A synthetic approach to research and practice*, (pp. 107–127). Washington, DC: Island Press.

Morris, J. T., Edwards, J., Crooks, S., & Reyes, E. (2012). Assessment of carbon sequestration potential in coastal wetlands. In *Recarbonization of the biosphere*, (pp. 517–531). Netherlands: Springer.

Morris, J. T., Sundareshwar, P. V., Nietch, C. T., Kjerfve, B., & Cahoon, D. R. (2002). Responses of coastal wetlands to rising sea level. *Ecology*, *83*(10), 2869–2877. https://doi.org/10.1890/0012-9658(2002)083[2869:ROCWTR]2.0.CO;2

Morris, J. T., Sundberg, K., & Hopkinson, C. S. (2013). Salt marsh primary production and its responses to relative sea level and nutrients in estuaries at Plum Island, Massachusetts, and North Inlet, South Carolina, USA. *Oceanography*, *26*(3), 78–84. https://doi.org/10.5670/oceanog.2013.48

Moseman-Valtierra, S., Abdul-Aziz, O. I., Tang, J., Ishtiaq, K. S., Morkeski, K., Mora, J., et al. (2016). Carbon dioxide fluxes reflect plant zonation and belowground biomass in a coastal marsh. *Ecosphere*, *7*(11), 1–21.

Myhre, G., Shindell, D., Bréon, F. M., Collins, W., Fuglestvedt, J., Huang, J., et al. (2013). Anthropogenic and natural radiative forcing. In T. F. Stocker et al. (Eds.), *Climate change 2013: The physical science basis. Contribution of Working Group I to the Fifth Assessment Report of the Intergovernmental Panel on Climate Change* (pp. 679–740). Cambridge, UK and New York: Cambridge University Press.

Nahlik, A. M., & Mitsch, W. J. (2011). Methane emissions from tropical freshwater wetlands located in different climatic zones of Costa Rica. *Global Change Biology*, *17*(3), 1321–1334. https://doi.org/10.1111/j.1365-2486.2010.02190.x

National Oceanic and Atmospheric Administration (NOAA). (2017). NOAA tides and currents data portal. Available online at https://tidesandcurrents.noaa.gov/stationhome.html?id=8447930. Last accessed on 27 December 2017.

National Research Council (2015). *Climate intervention: Carbon dioxide removal and reliable sequestration*. Washington, D. C: National Academies Press.

Nedwell, D., Embley, T. M., & Purdy, K. J. (2004). Sulphate reduction, methanogenesis and phylogenetics of the sulphate reducing bacterial communities along an estuarine gradient. *Aquatic Microbial Ecology*, *37*(3), 209–217. https://doi.org/10.3354/ame037209

Nellemann, C., & Corcoran, E. (Eds.) (2009). Blue carbon: The role of healthy oceans in binding carbon: A rapid response assessment. UNEP/Earthprint.

Neubauer, S. C., Miller, W. D., & Anderson, I. C. (2000). Carbon cycling in a tidal freshwater marsh ecosystem: A carbon gas flux study. *Marine Ecology Progress Series*, *199*, 13–30. https://doi.org/10.3354/meps199013

Parida, A. K., & Das, A. B. (2005). Salt tolerance and salinity effects on plants: A review. *Ecotoxicology and Environmental Safety*, *60*(3), 324–349. https://doi.org/10.1016/j.ecoenv.2004.06.010

Pearcy, R. W., & Ustin, S. L. (1984). Effects of salinity on growth and photosynthesis of three California tidal marsh species. *Oecologia*, *62*(1), 68–73. https://doi.org/10.1007/BF00377375

Pendall, E., Bridgham, S., Hanson, P. J., Hungate, B., Kicklighter, D. W., Johnson, D. W., et al. (2004). Below-ground process responses to elevated CO_2 and temperature: A discussion of observations, measurement methods, and models. *New Phytologist*, *162*(2), 311–322. https://doi.org/10.1111/j.1469-8137.2004.01053.x

Pierfelice, K. N., Graeme Lockaby, B., Krauss, K. W., Conner, W. H., Noe, G. B., & Ricker, M. C. (2015). Salinity influences on aboveground and belowground net primary productivity in tidal wetlands. *Journal of Hydrologic Engineering*, *22*(1), D5015002.

Poffenbarger, H. J., Needelman, B. A., & Megonigal, J. P. (2011). Salinity influence on methane emissions from tidal marshes. *Wetlands*, *31*(5), 831–842. https://doi.org/10.1007/s13157-011-0197-0

Potter, C. S. (1997). An ecosystem simulation model for methane production and emission from wetlands. *Global Biogeochemical Cycles*, *11*, 495–506. https://doi.org/10.1029/97GB02302

Ravit, B., Ehrenfeld, J. G., & Haggblom, M. M. (2003). A comparison of sediment microbial communities associated with Phragmites australis and Spartina alterniflora in two brackish wetlands of New Jersey. *Estuaries and Coasts*, *26*(2), 465–474. https://doi.org/10.1007/BF02823723

Roulet, N. T., Ash, R., & Moore, T. R. (1992). Low boreal wetlands as a source of atmospheric methane. *Journal of Geophysical Research*, *97*, 3739–3749. https://doi.org/10.1029/91JD03109

Ryan, M. G., & Law, B. E. (2005). Interpreting, measuring, and modeling soil respiration. *Biogeochemistry*, *73*(1), 3–27. https://doi.org/10.1007/s10533-004-5167-7

Sage, R. F. (2002). Variation in the k_{cat} of Rubisco in C_3 and C_4 plants and some implications for photosynthetic performance at high and low temperature. *Journal of Experimental Botany*, *53*(369), 609–620. https://doi.org/10.1093/jexbot/53.369.609

Sage, R. F., & Kubien, D. S. (2007). The temperature response of C_3 and C_4 photosynthesis. *Plant, Cell & Environment*, *30*(9), 1086–1106. https://doi.org/10.1111/j.1365-3040.2007.01682.x

Savage, V. M., Gillooly, J. F., Woodruff, W. H., West, G. B., Allen, A. P., Enquist, B. J., & Brown, J. H. (2004). The predominance of quarter-power scaling in biology. *Functional Ecology*, *18*(2), 257–282. https://doi.org/10.1111/j.0269-8463.2004.00856.x

Schedlbauer, J. L., Munyon, J. W., Oberbauer, S. F., Gaiser, E. E., & Starr, G. (2012). Controls on ecosystem carbon dioxide exchange in short-and long-hydroperiod Florida Everglades freshwater marshes. *Wetlands*, *32*(5), 801–812. https://doi.org/10.1007/s13157-012-0311-y

Schile, L. M., Callaway, J. C., Morris, J. T., Stralberg, D., Parker, V. T., & Kelly, M. (2014). Modeling tidal marsh distribution with sea-level rise: Evaluating the role of vegetation, sediment, and upland habitat in marsh resiliency. *PLoS One*, *9*(2), e88760. https://doi.org/10.1371/journal.pone.0088760

Schile, L. M., Callaway, J. C., Suding, K. N., & Kelly, N. M. (2017). Can community structure track sea-level rise? Stress and competitive controls in tidal wetlands. *Ecology and Evolution*, *7*(4), 1276–1285. https://doi.org/10.1002/ece3.2758

Schumann, S., Nolte, L. P., & Zheng, G. (2013). Comparison of partial least squares regression and principal component regression for pelvic shape prediction. *Journal of Biomechanics*, *46*(1), 197–199. https://doi.org/10.1016/j.jbiomech.2012.11.005

Schwefel, R., Hondzo, M., Wüest, A., & Bouffard, D. (2017). Scaling oxygen microprofiles at the sediment interface of deep stratified waters. *Geophysical Research Letters*, *44*, 1340–1349. https://doi.org/10.1002/2016GL072079

Seber, G. A. F., & Wild, C. J. (2003). *Nonlinear regression*. Hoboken, NJ: Wiley-Interscience.

Seber, G. A. F., & Wild, C. J. (2005). Computational methods for nonlinear least squares. In *Nonlinear regression*, (pp. 619–660). Hoboken, NJ, USA: John Wiley. https://doi.org/10.1002/0471725315.ch14

Segers, R. (1998). Methane production and methane consumption: A review of processes underlying wetland methane fluxes. *Biogeochemistry*, *41*(1), 23–51. https://doi.org/10.1023/A:1005929032764

Serran, J. N., & Creed, I. F. (2016). New mapping techniques to estimate the preferential loss of small wetlands on prairie landscapes. *Hydrological Processes*, *30*(3), 396–409. https://doi.org/10.1002/hyp.10582

Serran, J. N., Creed, I. F., Ameli, A. A., & Aldred, D. A. (2018). Estimating rates of wetland loss using power-law functions. *Wetlands*, *38*(1), 109–120. https://doi.org/10.1007/s13157-017-0960-y

Sharifi, A., Kalin, L., Hantush, M. M., Isik, S., & Jordan, T. E. (2013). Carbon dynamics and export from flooded wetlands: A modeling approach. *Ecological Modelling*, *263*, 196–210. https://doi.org/10.1016/j.ecolmodel.2013.04.023

Sierra, C. A. (2012). Temperature sensitivity of organic matter decomposition in the Arrhenius equation: Some theoretical considerations. *Biogeochemistry*, *108*(1–3), 1–15. https://doi.org/10.1007/s10533-011-9596-9

Silvestri, S., & Marani, M. (2004). Salt-marsh vegetation and morphology: Basic physiology, modelling and remote sensing observations. In S. Fagherazzi, M. Marani, & L. K. Blum (Eds.), *The Ecogeomorphology of Salt Marshes, Coastal Estuarine Studies* (Vol. 59, pp. 5–26). Washington, DC: American Geophysical Union. https://doi.org/10.1029/CE059p0005

Smith, K. A., Ball, T., Conen, F., Dobbie, K. E., Massheder, J., & Rey, A. (2003). Exchange of greenhouse gases between soil and atmosphere: Interactions of soil physical factors and biological processes. *European Journal of Soil Science*, *54*(4), 779–791. https://doi.org/10.1046/j.1351-0754.2003.0567.x

Song, C., Xu, X., Tian, H., & Wang, Y. (2009). Ecosystem–atmosphere exchange of CH_4 and N_2O and ecosystem respiration in wetlands in the Sanjiang Plain, Northeastern China. *Global Change Biology*, *15*(3), 692–705. https://doi.org/10.1111/j.1365-2486.2008.01821.x

Sposito, G. (Ed) (2008). *Scale dependence and scale invariance in hydrology*. Cambridge University Press.

St-Hilaire, F., Wu, J., Roulet, N. T., Frolking, S., Lafleur, P. M., Humphreys, E. R., & Arora, V. (2010). McGill wetland model: Evaluation of a peatland carbon simulator developed for global assessments. *Biogeosciences*, *7*(11), 3517–3530. https://doi.org/10.5194/bg-7-3517-2010

Stoy, P. C., Katul, G. G., Siqueira, M. B., Juang, J. Y., McCarthy, H. R., Kim, H. S., et al. (2005). Variability in net ecosystem exchange from hourly to inter-annual time scales at adjacent pine and hardwood forests: A wavelet analysis. *Tree Physiology*, *25*(7), 887–902. https://doi.org/10.1093/treephys/25.7.887

Tong, C., Wang, C., Huang, J. F., Wang, W. Q., Yan, E., Liao, J., & Yao, C. (2014). Ecosystem respiration does not differ before and after tidal inundation in brackish marshes of the Min River estuary, Southeast China. *Wetlands*, *34*(2), 225–233. https://doi.org/10.1007/s13157-013-0478-x

Tong, C., Wang, W. Q., Zeng, C. S., & Marrs, R. (2010). Methane (CH4) emission from a tidal marsh in the Min River estuary, Southeast China. *Journal of Environmental Science and Health Part A*, *45*(4), 506–516. https://doi.org/10.1080/10934520903542261

Tukey, J. W. (1977). *Exploratory data analysis*. Menlo Park, CA: Addison Wesley.

Turetsky, M. R., Kotowska, A., Bubier, J., Dise, N. B., Crill, P., Hornibrook, E. R., et al. (2014). A synthesis of methane emissions from 71 northern, temperate, and subtropical wetlands. *Global Change Biology*, *20*(7), 2183–2197. https://doi.org/10.1111/gcb.12580

United States Geological Survey (USGS). (2017). USGS Geo Data Portal. Available online at https://cida.usgs.gov/gdp/client/#!catalog/gdp/dataset/5752f2d9e4b053f0edd15628. Last accessed on 20 March 2017.

Valiela, I., Geist, M., McClelland, J., & Tomasky, G. (2000). Nitrogen loading from watersheds to estuaries: Verification of the Waquoit Bay nitrogen loading model. *Biogeochemistry*, *49*(3), 277–293. https://doi.org/10.1023/A:1006345024374

Van der Nat, F. J., & Middelburg, J. J. (2000). Methane emission from tidal freshwater marshes. *Biogeochemistry*, *49*(2), 103–121.

Van Huissteden, J., van den Bos, R., & Alvarez, I. M. (2006). Modelling the effect of water-table management on CO_2 and CH_4 fluxes from peat soils. *Netherlands Journal of Geosciences*, *85*(01), 3–18. https://doi.org/10.1017/S0016774600021399

Vasquez, E. A., Glenn, E. P., Guntenspergen, G. R., Brown, J. J., & Nelson, S. G. (2006). Salt tolerance and osmotic adjustment of *Spartina alterniflora* (Poaceae) and the invasive M haplotype of *Phragmites australis* (Poaceae) along a salinity gradient. *American Journal of Botany*, *93*(12), 1784–1790. https://doi.org/10.3732/ajb.93.12.1784

Vivanco, L., Irvine, I. C., & Martiny, J. B. (2015). Nonlinear responses in salt marsh functioning to increased nitrogen addition. *Ecology*, *96*(4), 936–947. https://doi.org/10.1890/13-1983.1

Walter, B. P., & Heimann, M. (2000). A process-based, climate-sensitive model to derive methane emissions from natural wetlands: Application to five wetland sites, sensitivity to model parameters, and climate. *Global Biogeochemical Cycles*, *14*, 745–765. https://doi.org/10.1029/1999GB001204

Wang, D., Chen, Z., & Xu, S. (2009). Methane emission from Yangtze estuarine wetland, China. *Journal of Geophysical Research*, *114*, G02011. https://doi.org/10.1029/2008JG000857

Wang, H., Hsieh, Y. P., Harwell, M. A., & Huang, W. (2007). Modeling soil salinity distribution along topographic gradients in tidal salt marshes in Atlantic and Gulf coastal regions. *Ecological Modelling*, *201*(3-4), 429–439. https://doi.org/10.1016/j.ecolmodel.2006.10.013

Wang, Q., Wang, C. H., Zhao, B., Ma, Z. J., Luo, Y. Q., Chen, J. K., & Li, B. (2006). Effects of growing conditions on the growth of and interactions between salt marsh plants: Implications for invasibility of habitats. *Biological Invasions*, *8*(7), 1547–1560. https://doi.org/10.1007/s10530-005-5846-x

Wang, Z. A., Kroeger, K. D., Ganju, N. K., Gonneea, M. E., & Chu, S. N. (2016). Intertidal salt marshes as an important source of inorganic carbon to the coastal ocean. *Limnology and Oceanography*, *61*(5), 1916–1931. https://doi.org/10.1002/lno.10347

Waquoit Bay National Estuarine Research Reserve (2014) Waquoit Bay National Estuarine Research Reserve Management Plan, 2014–2019. Available online at http://www.waquoitbayreserve.org/wp-content/uploads/WB-2014-2019-Management-Plan_Final.pdf

Warnaars, T. A., Hondzo, M., & Power, M. E. (2007). Abiotic controls on periphyton accrual and metabolism in streams: Scaling by dimensionless numbers. *Water Resources Research*, *43*, W08425. https://doi.org/10.1029/2006WR005002

Weston, N. B., Neubauer, S. C., Velinsky, D. J., & Vile, M. A. (2014). Net ecosystem carbon exchange and the greenhouse gas balance of tidal marshes along an estuarine salinity gradient. *Biogeochemistry*, *120*(1–3), 163–189. https://doi.org/10.1007/s10533-014-9989-7

Whalen, S. C. (2005). Biogeochemistry of methane exchange between natural wetlands and the atmosphere. *Environmental Engineering Science*, *22*(1), 73–94. https://doi.org/10.1089/ees.2005.22.73

Wigand, C., Brennan, P., Stolt, M., Holt, M., & Ryba, S. (2009). Soil respiration rates in coastal marshes subject to increasing watershed nitrogen loads in southern New England, USA. *Wetlands*, *29*(3), 952–963. https://doi.org/10.1672/08-147.1

Wilson, A. M., & Morris, J. T. (2012). The influence of tidal forcing on groundwater flow and nutrient exchange in a salt marsh-dominated estuary. *Biogeochemistry*, *108*(1–3), 27–38. https://doi.org/10.1007/s10533-010-9570-y

Wold, S., Sjöström, M., & Eriksson, L. (2001). PLS-regression: A basic tool of chemometrics. *Chemometrics and Intelligent Laboratory Systems*, *58*(2), 109–130. https://doi.org/10.1016/S0169-7439(01)00155-1

Xie, X., Zhang, M. Q., Zhao, B., & Guo, H. Q. (2014). Dependence of coastal wetland ecosystem respiration on temperature and tides: A temporal perspective. *Biogeosciences*, *11*(3), 539–545. https://doi.org/10.5194/bg-11-539-2014

Yurova, A., Wolf, A., Sagerfors, J., & Nilsson, M. (2007). Variations in net ecosystem exchange of carbon dioxide in a boreal mire: Modeling mechanisms linked to water table position. *Journal of Geophysical Research*, *112*, G02025. https://doi.org/10.1029/2006JG000342

Yvon-Durocher, G., Allen, A. P., Bastviken, D., Conrad, R., Gudasz, C., St-Pierre, A., et al. (2014). Methane fluxes show consistent temperature dependence across microbial to ecosystem scales. *Nature*, *507*(7493), 488–491. https://doi.org/10.1038/nature13164

Zhang, Y., Li, C., Trettin, C. C., Li, H., & Sun, G. (2002). An integrated model of soil, hydrology, and vegetation for carbon dynamics in wetland ecosystems. *Global Biogeochemical Cycles*, *16*(4), 1061. https://doi.org/10.1029/2001GB001838